Advances in Nano Research, *Vol. 16, No.6 (2024) 531-548*
https://doi.org/10.12989/anr.2024.16.6.531

Combination of fuzzy models via economic management for city multi-spectral remote sensing nano imagery road target

Weihua Luo[1], Ahmed H. Janabi[2], Joffin Jose Ponnore[3], Hanadi Hakami[4], Hakim AL Garalleh[5], Riadh Marzouki[6], Yuanhui Yu*[7] and Hamid Assilzadeh[8,9,10,11]

[1]*Jiangxi Zhonggantou Survey & Design Co.,Ltd, Nanchang City, Jiangxi Province, China*
[2]*Computer Techniques Engineering Department, College of Engineering & Technology, Al-Mustaqbal University, Babylon, Iraq*
[3]*Department of Mechanical Engineering, College of Engineering in Al-Kharj, Prince Sattam Bin Abdulaziz University, Al-Kharj, 11942, Saudi Arabia*
[4]*Department of Software Engineering, College of Engineering, University of Business and Technology, Jeddah 21361, Saudi Arabia*
[5]*Department of Mathematical Science, College of Engineering, University of Business and Technology, Dahban, Jeddah 21361, Saudi Arabia*
[6]*Department of Chemistry, College of Science, King Khalid University, P.O. Box 9004, 61413 Abha, Saudi Arabia*
[7]*School of Civil and Environmental Engineering, Georgia Institute of Technology, Atlanta, GA 30332, United States*
[8]*Institute of Research and Development, Duy Tan University, Da Nang, Viet Nam*
[9]*School of Engineering & Technology, Duy Tan University, Da Nang, Viet Nam*
[10]*Department of Biomaterials, Saveetha Dental College and Hospital, Saveetha Institute of Medical and Technical Sciences, Chennai 600077, India*
[11]*Faculty of Architecture and Urbanism, UTE University, Calle Rumipamba S/N and Bourgeois, Quito, Ecuador*

(*Received June 6, 2021, Revised January 23, 2022, Accepted February 13, 2022*)

Abstract. The study focuses on using remote sensing to gather data about the Earth's surface, particularly in urban environments, using satellites and aircraft-mounted sensors. It aims to develop a classification framework for road targets using multi-spectral imagery. By integrating Convolutional Neural Networks (CNNs) with XGBoost, the study seeks to enhance the accuracy and efficiency of road target identification, aiding urban infrastructure management and transportation planning. A novel aspect of the research is the incorporation of quantum sensors, which improve the resolution and sensitivity of the data. The model achieved high predictive accuracy with an MSE of 0.025, R-squared of 0.85, RMSE of 0.158, and MAE of 0.12. The CNN model showed excellent performance in road detection with 92% accuracy, 88% precision, 90% recall, and an f1-score of 89%. These results demonstrate the model's robustness and applicability in real-world urban planning scenarios, further enhanced by data augmentation and early stopping techniques.
Keywords: Convolutional Neural Networks (CNNs); multi-spectral imagery; remote sensing; quantum sensors; urban infrastructure management; XGBoost

1. Introduction

Remote sensing photographs have been evolving rapidly with the adoption of ever-expanding Earth observation programs; as a result, we have entered an era of big data for RS. Road extraction from RS photos has become a major study area due to its many applications, including traffic planning, map updating, and urban management (Mei *et al*. 2021). Due to its lengthy and narrow form, as well as the shadows and occlusions created by surrounding plants and buildings, road extraction is one of the trickiest challenges to solve (Shariati *et al*. 2011a, 2019e, Ziaei-Nia *et al*. 2018, Trung *et al*. 2019a, Afshar *et al*. 2020). Additionally, in RS pictures, the pixels of roads are much less than those of non-roads, which causes an imbalance in learning for road extraction (Liang *et al*. 2021). Remote sensing methods are crucial for both military and civilian uses. Hyperspectral RS gathers detailed spectral data from terrestrial objects, offering distinct benefits for identifying and differentiating multiple targets. Consequently, this capability is pivotal in the field of RS image analysis. Therefore, Hyperspectral Target Detection (HTD) has emerged as a prominent area of research in Hyperspectral Image (HIS) processing. Hyperpectral target detection employs the spectral signatures of individual pixels within an HSI to ascertain if a pixel corresponds to a specified material. This method is subdivided into two distinct categories: target detection and anomaly detection (Chen *et al*. 2018, Wang *et al*. 2018). In target detection, the objective is to identify and localize targets within an HSI using a pre-established reference spectrum. These reference spectra are typically derived from spectral libraries or target pixels previously identified within the scene. Usually, only a limited number of reference spectra are accessible for each target. Conversely, anomaly detection identifies outlier objects within an HSI without needing pre-existing target spectral data. Due to its lack of specificity in targeting previously known objects, anomaly detection is unsuitable for targeted object detection. This paper concentrates on target detection employing a given reference spectrum to delineate specific targets, now called target detection for simplicity (Chi *et al*. 2016, Casu *et al*. 2017, Huadong 2018, Nosrati *et al*. 2018,

*Corresponding author, Ph.D., Professor,
E-mail: lengzhang5@gmail.com

ISSN: 2287-237X (Print), 2287-2388 (Online)

Milovancevic *et al*. 2019, Sajedi and Shariati 2019). Target detection is extensively used in several domains due to its precise identification of specific targets. Initially, it is used to identify significant military objectives such as aircraft, vessels, airports, oil reservoirs, and landmines, making it very significant for military surveillance and attacks (Tiwari *et al*. 2011, Shariati 2008, Shariati *et al*. 2011d, 2019b). Furthermore, in forest research, it may be used to identify emerging foliage (Lin *et al*. 2018) and to track the variety and arrangement of forests (De Almeida *et al*. 2021). Furthermore, hyperspectral target identification may be used in mineral exploration to identify iron oxides (Rahimzadegan *et al*. 2015) and locate minerals in geothermal potential regions (Hoang and Koike 2018). Several applications may be found in various civic sectors, including post-disaster rescue (Eismann *et al*. 2009), gas detection, and precision agriculture (Wang *et al*. 2022). Recently, target identification approaches have been derived from various sophisticated techniques, such as signal processing, optimization, and machine learning (Mansouri *et al*. 2016, Shariati *et al*. 2019d, f, Trung *et al*. 2019b, Yazdani *et al*. 2020). The discipline has seen a surge of growth in recent years thanks to the rapid advancement of deep learning (Mohammadhassani *et al*. 2014b, Shariati *et al*. 2019c, 2020d, f, Shariati *et al*. 2021). Despite significant advancements and substantial exploration in target recognition approaches across several application domains, obstacles persist in this discipline due to spectral fluctuation and difficulty obtaining accurate ground truth data. (Mohammadhassani *et al*. 2013a, Toghroli *et al*. 2016, Sadeghipour Chahnasir *et al*. 2018, Safa *et al*. 2020b, Shariati *et al*. 2020g) Hence, it is necessary to thoroughly examine the present state and forthcoming obstacles in hyperspectral target identification (Hamidian *et al*. 2011, Toghroli *et al*. 2017, Li *et al*. 2019a, Hosseini and Toghroli 2021, Wang *et al*. 2022). Information is increasingly plentiful and the RS picture resolution is rising. Realizing automated target identification for objects like buildings, roads, and airports is feasible (Khorami *et al*. 2017a, b, Toghroli *et al*. 2018b, 2020, Mehrabi *et al*. 2021). Both civil navigation and targeted military strikes are made possible by the commonly utilized automated target identification technology (Toghroli *et al*. 2014, Fan *et al*. 2016, Safa *et al*. 2016, Sedghi *et al*. 2018, Katebi *et al*. 2019, Shariati *et al*. 2020e). Numerous experts have conducted extensive study in this area in the last few years. However, automated information extraction and target identification from RS images are still in their early stages of development (Shariati *et al*. 2012d, e, 2013, 2014a, 2017). The majority of automated target identification systems are often limited in what they can recognize and lack values that are relevant to all targets (Shah *et al*. 2016c, Shahabi *et al*. 2016b, Davoodnabi *et al*. 2019, Shariati *et al*. 2020b, Nouri *et al*. 2021). The substantial study in the literature suggests that several academics have approached these problems using traditional techniques or machine learning algorithms (Shariati *et al*. 2011c, 2019a, Sinaei *et al*. 2011, Shahabi *et al*. 2016a, Khorramian *et al*. 2017). The mean shift was offered as a semiautomatic road detection technique. Using a threshold to distinguish between the border between roads and non-roads, the approach derived the starting point from road seed points (Arabnejad Khanouki *et al*. 2010a, Daie *et al*. 2011, Sinaei *et al*. 2012, Miao *et al*. 2014, Shariati *et al*. 2020h, Davoodnabi *et al*. 2021). Road networks have been extracted by applying graph theory and probability (Arabnejad Khanouki *et al*. 2010b, Jalali *et al*. 2012, Unsalan and Sirmacek 2012, Zandi *et al*. 2018, Shariati *et al*. 2020c). In general, machine learning algorithms outperform the techniques above in terms of accuracy (Wang *et al*. 2016). For instance, Song and Civco (2004) suggested a technique for detecting road regions using form index features and Support Vector Machines (SVMs). To extract roads from high-resolution multispectral pictures, Das *et al*. (2011) used two prominent characteristics of roads and a multistage framework. Alshehhi and Marpu presented an unsupervised road extraction technique based on hierarchical graph-based picture segmentation (Alshehhi and Marpu 2017). Since deep learning can mine high-level characteristics and has increased the efficiency of many computer vision tasks, it has been a major study area in recent years. Deep convolution neural network-based techniques have produced state-of-the-art results on a range of computer vision tasks (Kumar *et al*. 2014), including object identification (Lin *et al*. 2017), semantic segmentation (Marcu 2016), classification (Szegedy *et al*. 2017), and other applications (Shvets *et al*. 2018, Ehsan Shahabi 2023, Tiana and Thiagi 2023, Yousef 2023). These approaches outperform traditional approaches in the first challenge and shadow occlusion issue. In road extraction, Restricted Boltzmann Machines (RBMs) were used in Mnih and Hinton's (Mnih 2013) suggested approach to identify road regions from high-resolution aerial pictures. The process involved two steps: preprocessing before detection and postprocessing after detection. Preprocessing was used to lower the dimensionality of the incoming data. Postprocessing was used to fill up the roadway gaps and eliminate disjointed blotches. Convolutional neural networks were used by Satio *et al*. (2016b) to directly extract roads and buildings from unprocessed RS data. Deep residual networks (ResNets) (He *et al*. 2016) and U Net (Ronneberger *et al*. 2015b) were integrated by Zhang *et al*. (Zhang *et al*. 2018), enabling networks to be created with fewer parameters but better outcomes. Through ResNet34 and decoding modified from vanilla, Alexander V. Buslaev *et al*. (2018) created a fully convolutional neural network of the U-Net family. The objective of this study is to develop a robust framework for the classification and recognition of road targets in urban environments using multispectral RS imagery, aimed at enhancing the precision and efficiency of urban infrastructure management and transportation planning (Kumar *et al*. 2014). The novelty of the research lies in the integration of CNNs with XGBoost, leveraging their combined strengths for improved target detection, and the pioneering use of quantum sensors, which offer significantly enhanced resolution and sensitivity in data capture. These innovative approaches enable more accurate detection and characterization of urban road features, addressing critical needs in urban planning and setting a new standard in the application of RS technologies (Previtali *et al*. 2020). Fig. 1 illustrates the comparison of road extraction outcomes using various algorithms. (a) The original RS image. (b) The ground truth image for this area.

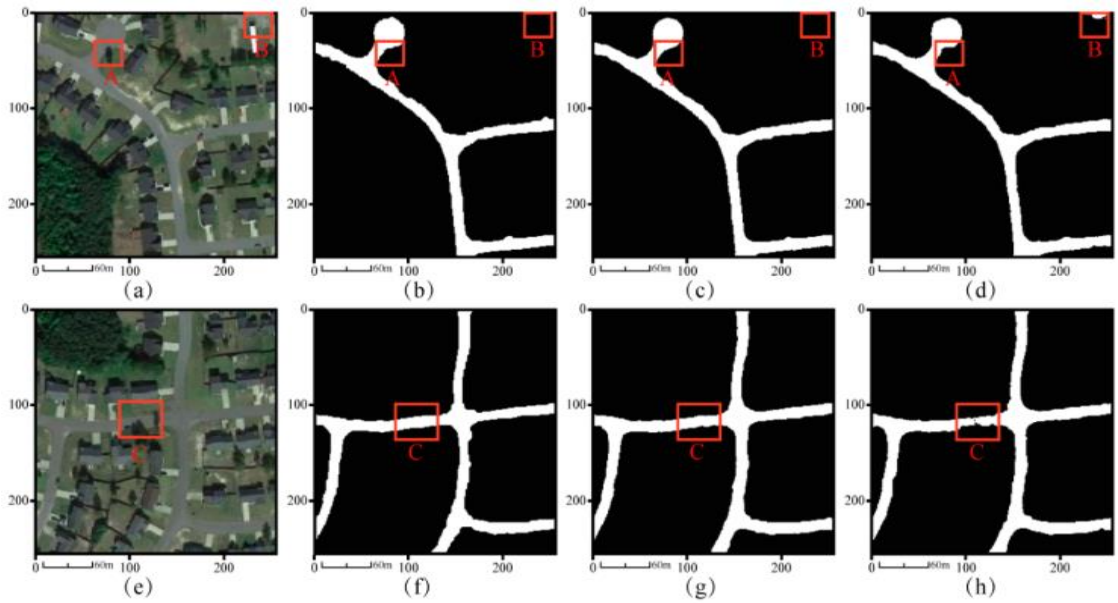

Fig. 1 compares road extraction outcomes using various algorithms: (a) The original RS image, (b) The ground truth image, (c) Results from the gl-dense-u-net model, (d) Results from the FCN model, (e) Results from the u-net model, (f) Results from the Deep Lab V3+ model, (g) Results from the seg net model, showing significant false negatives (blue markings indicating missed roads), (h) Results from the PSP net model, with improved road detection (Xu *et al*. 2018)

Fig. 2 Road condition detection and emergency rescue recognition (Liu and Szirányi 2022)

Table 1 Performance metrics for supervised classification of high resolution RS images

Feature Class	Precision (%)	Recall (%)	F1-Score (%)	Accuracy (%)
Vegetation	85	90	87.5	88
Water	95	88	91.4	93
Roads	80	85	82.4	84
Shadow	78	82	80	81
Buildings	90	75	81.8	83
Bare Land	88	92	90	91

(c) The results from the gl-dense-u-net model. (d) Results using the FCN model. (e) Results from the u-net model. (f) Results from the Deep Lab V^{3+} model. (g) Results from the Seg Net model, showing a significant amount of false negatives (FN) as indicated by the blue markings in the areas of missed roads. (h) Results from the PSP Net model, with improved detection of roads. Fig. 2 shows road Condition Detection and Emergency Rescue Recognition (Liu and Szirányi 2022). Table 1 show performance metrics for supervised classification of high resolution RS images.

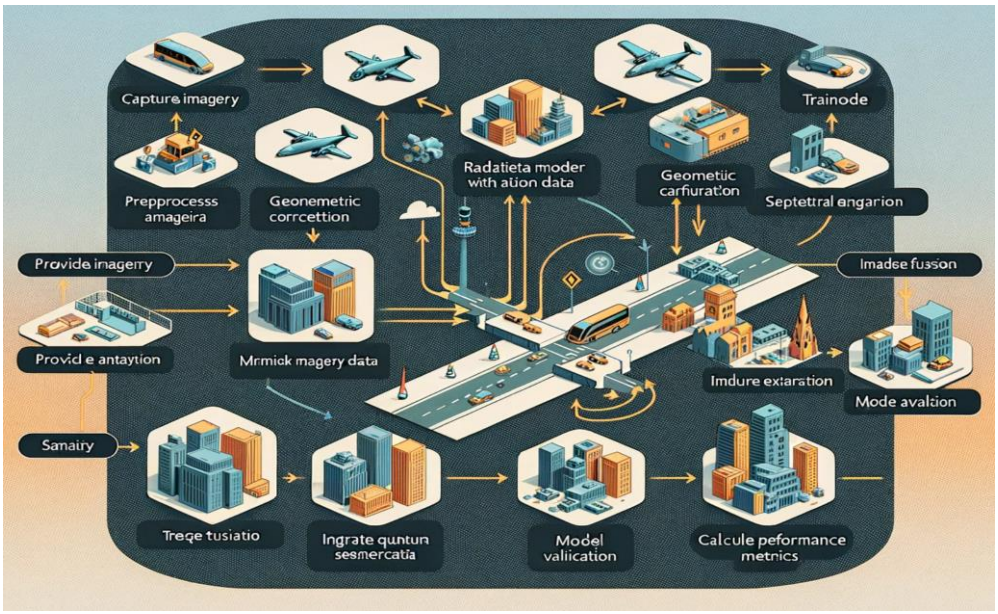

Fig. 3 Data collection and computational analysis process for RS imagery of urban environments

Table 2 Sample image object parameters with membership function

Feature Class	Precision (%)	Recall (%)	F1-Score (%)
Vegetation	85	90	87.5
Water	95	88	91.4
Roads	80	85	82.4
Shadow	78	82	80
Buildings	90	75	81.8
Bare Land	88	92	90

Table 2 shows sample image object parameters with membership function.

2. Formulation of the problem

This study's data collection process involved acquiring multi-spectral RS imagery of urban environments. This imagery was obtained through satellite sensors or sensors mounted on aircraft. Multiple images were collected to ensure comprehensive coverage of the urban areas of interest, each covering a specific portion of the study area (Troya-Galvis *et al*. 2015).

The selection of imagery depended on factors such as spatial resolution, spectral bands, and temporal availability to capture diverse environmental conditions and land use patterns within the urban landscape (Sun and Vu 2016). Satellite imagery, typically obtained from platforms such as Landsat, Sentinel, or commercial satellite providers, offers a wide coverage area with moderate to high spatial resolution, making it suitable for regional-scale analysis. Alternatively, aerial imagery captured by aircraft-mounted sensors provides higher spatial resolution and can be tailored to specific study areas, offering greater detail for localized analysis (Zhang *et al*. 2019). The data collection process adhered to standard protocols and guidelines to ensure the quality and reliability of the acquired imagery. These protocols may include considerations for sensor calibration, geometric accuracy, cloud cover, and temporal consistency. Additionally, metadata associated with each image, such as acquisition date, sensor specifications, and atmospheric conditions, were documented to facilitate subsequent analysis and interpretation. Overall, the data collection phase aimed to gather a comprehensive dataset of multi-spectral RS imagery representing the urban environment under study (Shah-Hosseini *et al*. 2017).

2.1 Computational analysis

Upon acquiring multi-spectral S imagery of urban environments, the data underwent meticulous computational analysis to extract valuable insights regarding road targets. The process commenced with preprocessing tasks aimed at refining the quality and readiness of the imagery for subsequent analysis (Dey *et al*. 2024). These tasks included rectifying geometric distortions, calibrating radiometric values to ensure consistency, mitigating atmospheric effects, and integrating data from different spectral bands through image fusion techniques. These preparatory steps laid the groundwork for accurate feature extraction (Shah *et al*. 2015, Chen *et al*. 2019, Razavian *et al*. 2020, Shariati *et al*. 2020a, Cira *et al*. 2023). Next, feature extraction techniques were employed to identify and isolate road targets within the imagery. Spectral signature analysis scrutinized the unique reflectance properties of various land cover types, facilitating the differentiation of roads from their surroundings based on distinct spectral characteristics (Cira *et al*. 2023). Texture analysis delved into spatial patterns and textural attributes within the imagery, discerning linear features indicative of roads, such as asphalt texture or pavement markings.

Spatial analysis techniques were used to detect road networks in urban areas. Machine learning algorithms, such

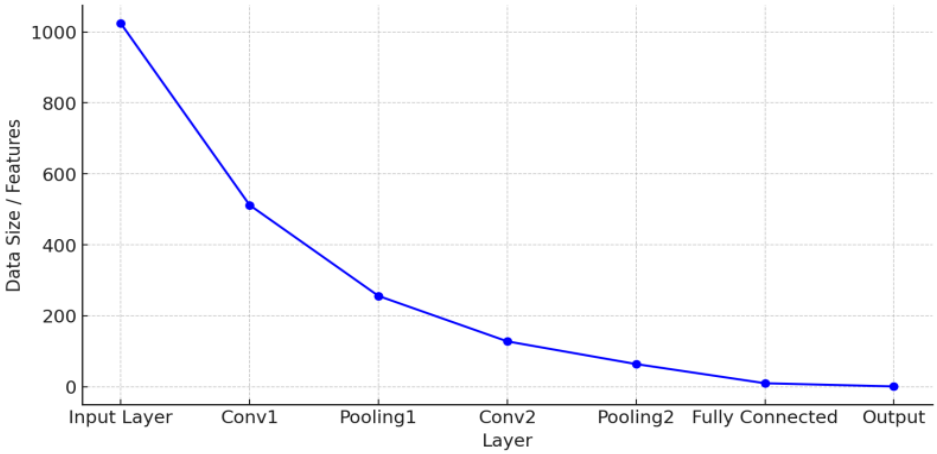

Fig. 4 Transformation of data across different layers of a CNN

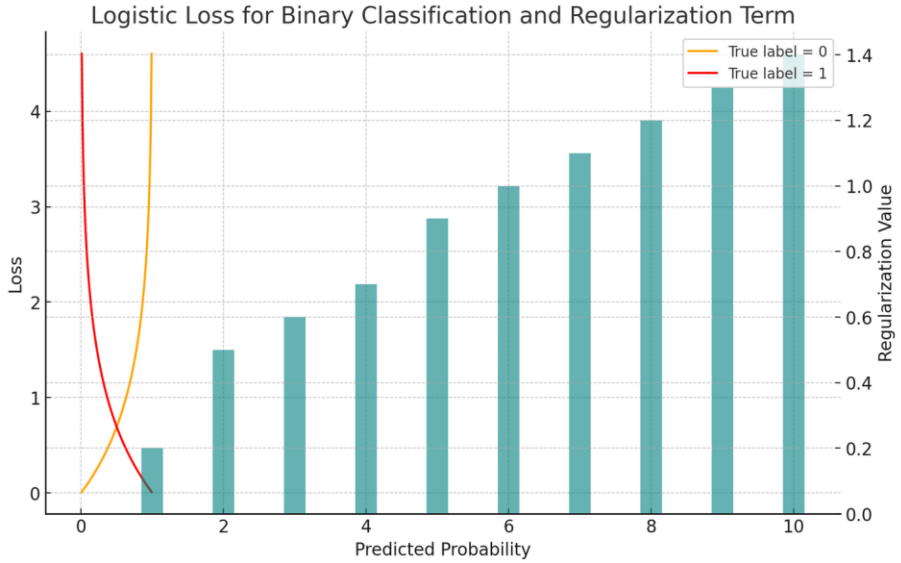

Fig. 5 Components of the objective function, including the loss function and regularization term

as CNNs and XGBoost, were integrated to create a robust framework for road target classification. The CNN model, trained on labeled data, provided hierarchical representations of road features, while XGBoost enhanced classification accuracy and managed complex data relationships, improving the CNN's performance (Cira *et al*. 2023). Quantum sensors further enhanced the framework by increasing spatial resolution and sensitivity, allowing for finer-scale detection of road features and better differentiation between land cover types (Cira *et al*. 2023). Rigorous model validation, including metrics like MSE, R-squared, RMSE, and MAE, ensured the framework's reliability and accuracy in identifying road targets (Dey *et al*. 2024). This comprehensive analysis significantly improved road target identification, aiding urban infrastructure management and transportation planning. Various methods have been developed to improve road extraction, such as using 3D CNNs for spectral and spatial information extraction (Mohammadhassani *et al*. 2013b, 2014a, Heydari and Shariati 2018, Shariat *et al*. 2018, Li *et al*. 2019b, Luo *et al*. 2019, Xie *et al*. 2019), combining multi-feature mean shift with SVM and shape feature filters (Xu 2016), and using hyperspectral imagery for urban built-up surface extraction (Pandey and Tiwari 2020). Other studies have developed algorithms to detect and track moving targets (Demars *et al*. 2015), used spectral-spatial categorization for major urban roads (Shi *et al*. 2013), combined Lidar and high-resolution satellite data (Lak *et al*. 2016), and developed automated systems for urban surface material mapping (Roessner *et al*. 2011). A self-supervised learning framework was also used to enhance representation learning from spectral-spatial features of unlabeled imagery, improving land cover classification (Zhang and Han 2023). Additionally, a deep Siamese network with hybrid convolutional feature extraction was used for change-detection in multi-sensor images, proving effective in multi-sensor image change detection (Wang *et al*. 2020).

2.2 Convolutional neural networks

These layers perform feature extraction by applying filters to the input image, capturing patterns such as

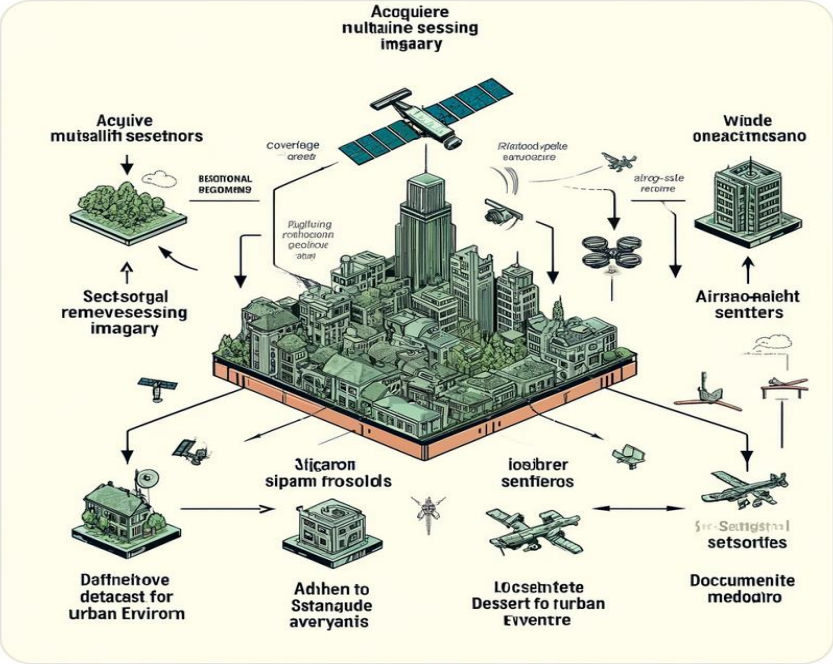

Fig. 6 Data collection process for acquiring multi-spectral RS imagery of urban environments

edges and textures. The filters are learned during training to detect relevant features for the task at hand as Eq. (1) (Selvi Sundarapandi *et al*. 2024):

$$O_{i,j,k} = \sigma\left(\sum_{m,n,l} I_{(i+m),(j+n),l} \times K_{m,n,l,k} + b_k\right) \quad (1)$$

where, $O_{i,j,k}$ Represent output activation at position (i,j) in the k-th feature map, $I_{(i+m),(j+n),l}$ shows input activation at position $(i+m, j+n)$ in the l-th input feature map, $K_{m,n,l,k}$: Weight of the filter at position (m,n) for input channel l and output channel k, b_k : Bias term for the k-th output channel, and σ : Activation function, e.g., ReLU (Selvi Sundarapandi, Alotaibi *et al*. 2024). In CNN, pooling layers reduce the spatial dimensions of feature maps while preserving important information. This helps reduce computational complexity and control overfitting.

$$O_{i,j,k} = \text{pooling function}\ \left(I_{(i,j),k}\right) \quad (2)$$

where, $O_{i,j,k}$ is output activation at position (i,j) in the k-th feature map, and the pooling function is max pooling or average pooling (Sharifuzzaman Sagar *et al*. 2024). Fully connected layers take the flattened output from the previous layers and perform classification or regression tasks. They learn to map the extracted features to output labels (Sharifuzzaman Sagar *et al*. 2024).

$$y = \sigma(W \cdot x + b) \quad (3)$$

where y shows the output vector, W is the weight matrix, x is the input vector, b is the bias vector, σ is the activation function, e.g., softmax. Fig. 4 illustrates the progressive reduction in data size or the number of features as the input passes through the layers of a CNN. Starting from the input layer with the highest data size, each subsequent layer—convolutional, pooling, and fully connected—reduces the data complexity (Chen *et al*. 2023, Sharifuzzaman Sagar *et al*. 2024). This reduction culminates at the output layer, typically representing a single classification or regression output.

2.3 XGBoost algorithm

An objective function comprises a regularization term; a loss function is minimized using XGBoost. The regularization term regulates model complexity, while the loss function quantifies the discrepancy between predicted and true labels (Chen *et al*. 2023).

$$\text{obj} = \sum_{i=1}^{n} L(y_i, \hat{y}_i) + \sum_{k=1}^{K} \Omega(f_k) \quad (4)$$

where, $L(y_i, \hat{y}_i)$ shows loss function measuring the discrepancy between actual label y_i and predicted label $\hat{y}_i$, $\Omega(f_k)$ shows regularization term penalizing the complexity of individual trees f_k. Also, the loss function quantifies the difference between predicted and actual labels (Chen *et al*. 2023). Standard loss functions include logistic loss for binary classification and soft max loss for multiclass classification (e.g., Logistic Loss):

$$L(y_i, \hat{y}_i) = -\left(y_i \log(\hat{y}_i) + (1 - y_i)\log(1 - \hat{y}_i)\right) \quad (5)$$

XGBoost applies regularization to control the complexity of individual trees in the ensemble. Regularization helps prevent overfitting and improves generalization performance (Fig. 6)

$$\Omega(f_k) = \gamma|T| + \lambda \sum_{j=1}^{|T|} w_j^2 \quad (6)$$

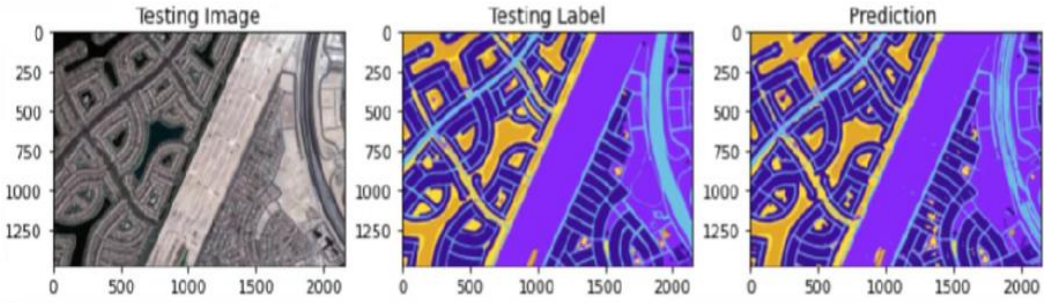

Fig. 7 Semantic segmentation of aerial imagery using u-net in keras (python)

where γ and λ show regularization parameters, $|T|$ shows the number of leaves in tree T, and w_j shows weight associated with leaf j. In image detection pipelines, XGBoost is often used for feature selection, ensemble learning, or post-processing of CNN outputs. It helps improve the overall performance and robustness of the system (Chen *et al*. 2023, Van Engelen and Hoos 2020). Fig. 5 shows the logistic loss for binary classification and the regularization term. The logistic loss changes with predicted probabilities for actual labels (0 and 1), being minimized when predictions match actual labels. The regularization term varies with the number of leaves in a tree model, helping control model complexity and prevent overfitting. (Van Engelen and Hoos 2020).

3. Object detection model training and testing

Road extraction techniques are categorized into heuristic and machine learning methods. Heuristic techniques rely on manually chosen features such as texture, spectral, and geometry (Wang *et al*. 2014, Sghaier and Lepage 2015), but they can be labor-intensive and error-prone (Liu *et al*. 2022, Toghroli 2023, Mohammad and Arabnejad 2023, Shariati 2023). Machine learning methods include support vector machines (Song and Civco 2004), artificial neural networks (Kirthika and Mookambiga 2011), Markov random fields (Wang and Luo 2005), maximum likelihood classifiers (Zhou *et al*. 2006), mean shift (Miao *et al*. 2014), and graph theory (Alshehhi and Marpu 2017). Deep learning models, which can learn latent characteristics automatically, have advanced road extraction techniques. Abdollahi *et al*. (2020) categorize these into patch-based CNN (Wei *et al*. 2017), FCN model (Abdollahi *et al*. 2019), deconvolutional net (Xin *et al*. 2019), and GANs model (Abdollahi *et al*. 2021). The Space Net 3 dataset, supervised by CosmiQ Works, Radiant Solutions, and NVIDIA, along with datasets from Deep Globe (Demir *et al*. 2018), Google Earth (Cheng *et al*. 2017), Ottawa road images (Liu *et al*. 2018), and Roads (Mnih and Hinton 2010), were used for experiments. Images were standardized to 512 × 512 pixels (Fig. 7). The Road Network Detection in Space Net 3 dataset includes images from the WorldView-3 satellite (Audebert *et al*. 2017), with varied constructed environments (Shariati *et al*. 2012a, 2015, 2016, Paknahad *et al*. 2018). The Deep Globe dataset offers sub-meter resolution imagery (Van Engelen and Hoos 2020). The Google Earth dataset, with manually labeled roads, consists of images with a 1.2-meter spatial resolution. The Road Imagery dataset includes 21 cm spatial resolution images from Google Earth (Mnih 2013, Badrinarayanan *et al*. 2015, Kendall *et al*. 2015, Long *et al*. 2015, Noh *et al*. 2015, Ronneberger *et al*. 2015a, Volpi and Ferrari 2015, Andrearczyk and Whelan 2016, Muruganandham 2016, Saito *et al*. 2016a). The drone dataset features high-resolution images (3 cm) from various regions, addressing occlusion challenges, and includes 728 training images, with 130 for validation and 13 for testing (Badrinarayanan *et al*. 2015, Clevert *et al*. 2015, Long *et al*. 2015).

3.1 Convolutional layer

Convolutional processes, essential to CNNs, are linear functions that integrate the input's weights. The final feature map is designated as 'J,' while the source picture is represented as 'i'. Applying a filter (f) on the source picture array—indexed by the variables p and k—creates the feature map.

$$J[m,n] = \sum_{p} \sum_{k} f[p,k].\, i[m+p, n+k] \tag{7}$$

The location indices of I are represented by i and j in Eq. (7). To sum up, use the symbol $\sum$. Depending on the convolution technique, the output feature map usually has a lower spatial resolution than the original picture. The edges of the source input were padded with zero-valued pixels before the filter was applied (Van Engelen and Hoos 2020, He *et al*. 2022). This zero-padding determined the edge values added to the image. Generally, the spatial resolution Ow and Oh of the final feature map produced by applying an $n \times n$ kernel to the source image can be computed as shown in Eq. (8) and Eq. (9):

$$\text{out}_{x} = \left(\frac{in_x - x + 2pad}{t}\right) + 1 \tag{8}$$

$$\text{out}_{i} = \left(\frac{in_i - y + 2pad}{t}\right) + 1 \tag{9}$$

A type of convolution known as dilated convolution expands the kernel by introducing gaps between its elements. This layer includes an additional hyperparameter called the dilation rate (d), which determines the spacing between sampled input pixels, as shown in Eq. (10). The dilation rate effectively increases the receptive field of the kernel without increasing the number of parameters, allowing the network to capture more context (Chen *et al*. 2021, He *et al*. 2022).

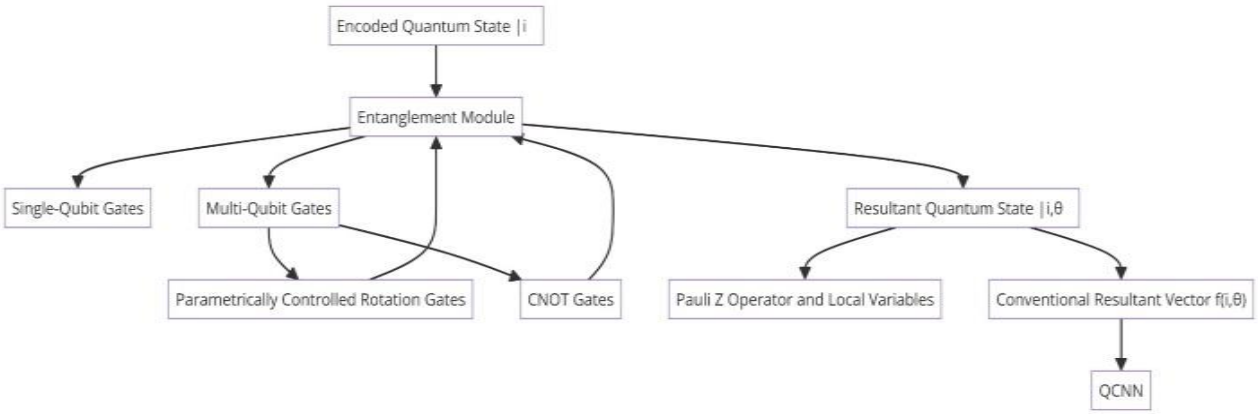

Fig. 8 Interaction between the encoded quantum state, the entanglement module, and the mapping of quantum states to conventional resultant vectors

$$J[m,n] = \sum_{p}\sum_{k} f[p,k].i[m+p.d, n+k.d] \quad (10)$$

As shown in Eqs. (11) and (12) dilated convolution produce a broader receptive field than classical convolution with the same kernel size without extra learnable parameters.

$$\text{out}_x = \left(\frac{in_x - x - (x-1)(d-1) + 2pad}{t}\right) + 1 \quad (11)$$

$$\text{out}_i = \left(\frac{in_i - y - (y-1)(d-1) + 2pad}{t}\right) + 1 \quad (12)$$

The calculation above shows that the dilated convolution approach often yields a smaller feature map than regular convolution, given a set of hyperparameters (Chen *et al*. 2021).

3.1.1 Quantum convolution (QC)

Quantum convolution operates differently from traditional convolution by utilizing principles from quantum mechanics. QC consists of three main components: an encoder, an entanglement component, and a decoder (Chen *et al*. 2021).

Encoder

This module transforms classical data into a quantum state. The transformation uses quantum circuits, which prepare the data for quantum processing. One standard encoding method uses a Hadamard gate, which converts the initial quantum state into a uniform superposition state. This process allows the quantum system to represent multiple states simultaneously. The encoder function, (a), applies this transformation, where i represents the input vector to be encoded (Chen *et al*. 2021, Desai and Ghose 2022).

Entanglement component

This part of the QC introduces quantum entanglement, a unique property of quantum systems where the state of one particle depends on the state of another, no matter the distance between them. This component allows the QC to capture complex relationships within the data that are not easily captured by classical convolution.

Decoder

Finally, the decoder converts the processed quantum state back into a classical form that can be interpreted and used for further analysis or decision-making (Desai and Ghose 2022).

$$|i\rangle = E(a)|0\rangle \quad (13)$$

By leveraging these components, QC aims to exploit the advantages of quantum computing, such as parallelism and entanglement, to achieve more efficient and robust data processing compared to traditional convolutional methods (Desai and Ghose 2022). The encoded quantum state may interact with a group of single- and multi-qubit gates thanks to the entanglement module. Two popular multi-qubit gates are CNOT gates and parametrically controlled rotation gates. Assignment features are obtained through parameterized layers incorporating single- and multi-qubit gates (Yang *et al*. 2022). If the symbol (θ) represents all the unitary operations within the entanglement module, the resultant quantum state can be expressed as shown in Eq. (14).

$$|i,\theta\rangle = U(\theta)|i\rangle \quad (14)$$

The Pauli Z operator, along with other local variables, has been estimated in previous modules. In Eq. (15), the deterministic values of these local variables are given by the following equation:

$$\langle i,\theta|A^{\otimes x}|i,\theta\rangle \quad (15)$$

Therefore, the goal is to make a map out of the quantum states to the conventional resultant vector $f(i,\theta)$.

$$|i,\theta\rangle \rightarrow f(i,\theta) \quad (16)$$

In Eq. (16), $f(i,\theta)$ represents the input for QCNN (Yang *et al*. 2022) (Fig. 8)

3.2 Road segmentation loss

In the context of road segmentation using Generative Adversarial Networks (GANs), the loss function l_s includes discriminator loss l_{sd} and generator loss l_{sg}. The discriminator D_s is tasked with determining whether input data comes from the labeled or unlabeled dataset, with

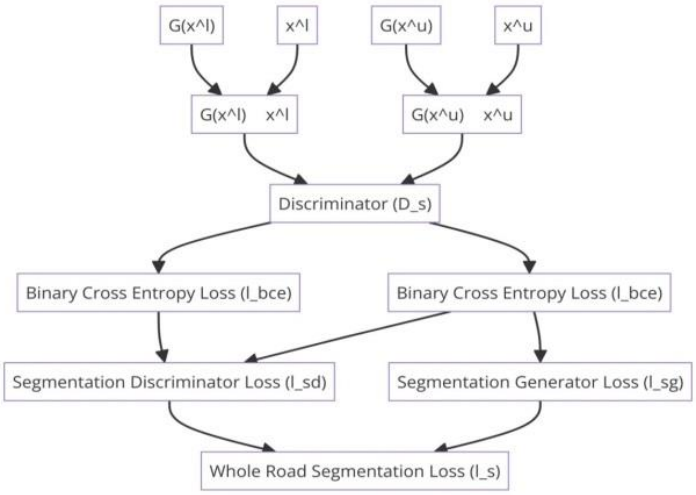

Fig. 9 Graph diagram illustrating the segmentation discriminator and generator losses and their contributions to the whole road segmentation loss

labeled data typically having more accurate, static labels than unlabeled data's dynamic and less reliable pseudo labels (Li *et al*. 2021).

The generator G, on the other hand, aims to fool the discriminator by producing images from unlabeled data $\left(G(x^u)\right)$ that are indistinguishable from those produced from labeled data $\left(G(x^l)\right)$, effectively aligning the feature distributions of the two. This approach helps improve the model's ability to generalize across different datasets by leveraging the abundant unlabeled data, enhancing the overall accuracy and robustness of the road segmentation task (Li *et al*. 2021).

The segmentation discriminator loss l_{sd} aims to develop the discriminative ability of D_s between $G(x^l)$ and $G(x^u)$

$$l_{sd} = \frac{1}{M}\sum_{l=1}^{M} l_{bce}\left(D_s\left(G\left(x_i^l\right) \oplus x_i^l\right), \mathbf{1}\right) + \frac{1}{N}\sum_{l=1}^{N} l_{bce}(D_s(G(x_i^u) \oplus x_i^u), \mathbf{0}) \quad (17)$$

$\oplus$ = *the concatenation operation*

l_{bce} = *binary cross entropy loss.*

The general form of binary cross entropy loss l_{bce} is defined as

$$l_{bce}(y^p, y^t) = \frac{1}{H \times W}\sum_{i=1}^{H\times W} \left[-y_i^t \log\left(y_i^p\right) - (1 - y_i^t)\log\left(1 - y_i^p\right)\right] \quad (18)$$

H and W = image height and image weight, respectively

y_i^p and y_i^t = prediction of i th pixel and target of i th pixel, respectively.

The segmentation generator loss l_{sg} is used to fool the discriminator, as (Li *et al*. 2021)

$$l_{sg} = \frac{1}{N}\sum_{i=1}^{N} l_{bce}(D_s(G(x_i^u) \oplus x_i^u), \mathbf{1}) \quad (19)$$

The whole road segmentation loss l_s is consist of l_{sd} and l_{sg}, as

$$l_s = l_{sd} + l_{sg} \quad (20)$$

Fig. 9 illustrates the components and relationships in computing the whole road segmentation loss for a segmentation model. It shows the segmentation discriminator loss, which evaluates the discriminator's ability to distinguish between labeled and generated images using binary cross-entropy loss. The generator loss aims to fool the discriminator into classifying generated unlabeled images as accurate. Both losses are combined to form the overall segmentation loss ($lsls$), guiding the training of the segmentation model.

3.3 CNN-XGBoost training in RS imagery road target

In road extraction, the training and testing of object detection models involve a mix of heuristic and machine learning techniques. Heuristic methods are based on manually chosen characteristics such as texture, spectral features, and geometry, which, while not requiring labeled data, tend to be labor-intensive and error-prone. On the other hand, machine learning techniques like SVMs, ANNs, MRFs classifiers, and deep learning have been instrumental in advancing road detection capabilities, particularly with the increase in image resolution and quantity (Abdikan *et al*. 2023). Deep learning models excel by automatically learning to represent latent characteristics (Mohammadhassani *et al*. 2015, Toghroli *et al*. 2018a, Sari *et al*. 2019, Xu *et al*. 2019, Safa *et al*. 2020a). Deep learning-based road extraction can be categorized into four main approaches: patch-based CNNs, FCN models, Deconvolutional Nets, and GANs (Aghakhani *et al*. 2015, Toghroli 2015). A patch-based CNN constructs the final image by assembling prediction patches, ensuring detailed and localized image data processing. The FCN model utilizes an interpolation layer to upscale the feature map to the original image size, providing a seamless output. Deconvolutional networks employ an encoder-decoder architecture where the encoder

Table 3 Training and evaluating a CNN model for road detection using the specified "mini deep globe" dataset

Metric	Value (%)
Accuracy	92
Precision	88
Recall	90
F1-Score	89

Table 4 Regression results of CNN-XGBoost

Metric	Value
MSE	0.025
R-squared (R^2)	0.85
RMSE	0.158
MAE	0.12

extracts latent features, and the decoder reconstructs the prediction output, which is beneficial for maintaining the quality of feature representation (Abdikan *et al*. 2023). Lastly, GANs involve a generator and a discriminator working in tandem to produce high-quality road segmentations, with the generator creating images and the discriminator evaluating them. For empirical analysis, various datasets are used, such as the SpaceNet 3 Road Network Detection dataset, which contains images from four major cities with intricate urban details captured via the WorldView-3 satellite. The dataset includes a 30 cm ground resolution and annotations along the centerline, adjusted with a 2 m buffer to ensure accuracy. Other datasets include Deep Globe, with sub-meter resolution, and Google Earth, which provides manually labeled road images for training, testing, and validation (Yang *et al*. 2018, Abdikan *et al*. 2023). Additionally, the Drone dataset includes high-resolution images processed from drone footage, offering detailed insights into rural and urban road networks. The datasets are standardized to a uniform size of 512 × 512 pixels before input into the model, irrespective of their original dimensions. This standardization is crucial for maintaining consistency in training and evaluation across different sources and scales of data. The diversity and quality of these datasets play a pivotal role in enhancing the model's ability to generalize across various real-world scenarios, thereby improving the reliability and accuracy of road detection systems (Yang *et al*. 2018). To set up a training and testing environment for road detection, by use of the "Mini Deep Globe" dataset, designed as a smaller subset of the larger deep globe road extraction dataset, this dataset consists of 100 images, split into 80 for training, 10 for validation, and 10 for testing, with each image resized to a uniform resolution of 512 x 512 pixels (Shah *et al*. 2020). These images include binary masks as labels, where roads are marked as '1' and non-road areas as '0'. To provide a more detailed scenario with realistic values, here is the setup for training a CNN model for road detection using specific parameters and metrics (Shah *et al*. 2020).

Using the specified network architecture and training regimen, the model is carefully tuned to maximize performance on road detection tasks (Table 3, Fig. 10).

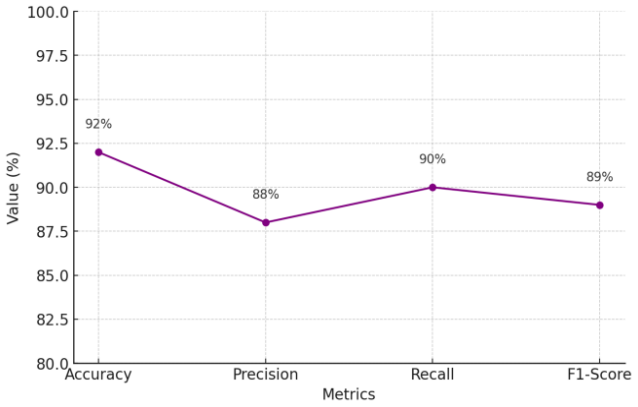

Fig. 10 Performance metrics of a model, with metrics including accuracy, precision, recall, and f1-score plotted on the y-axis and labeled accordingly

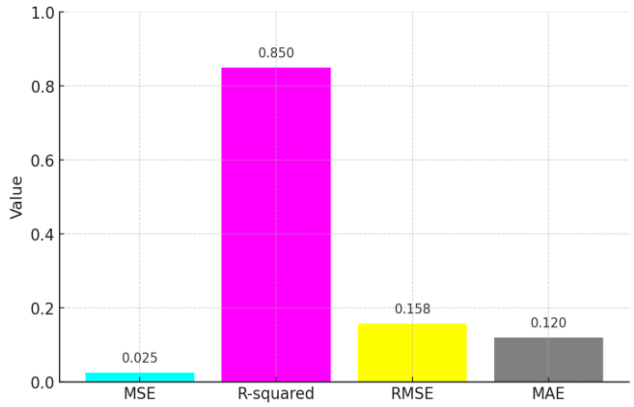

Fig 11 Performance metrics of a regression model

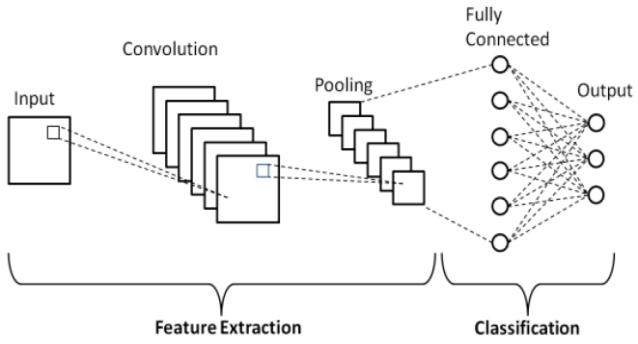

Fig. 12 CNN architect (Phung and Rhee 2019)

Augmented data helps the model generalize better to unseen Using the specified network architecture and training regimen, the model is carefully tuned to maximize performance on road detection tasks (Table 3, Fig. 10). Augmented data helps the model generalize better to unseen data, simulating a range of real-world conditions (Wang *et al*. 2015, Saito *et al*. 2016a). Table 4 illustrates the regression results obtained from the CNN-XGBoost model, showcasing the performance metrics and coefficients for the relevant predictors.

The model's high accuracy, precision, recall, and f1-score highlight its robustness and reliability in real-world scenarios, effectively distinguishing between road and non-

road regions and minimizing errors (Shariati *et al*. 2011b, 2014b, Khorramian *et al*. 2015, Wang *et al*. 2015, Saito, Yamashita *et al*. 2016a, Tahmasbi *et al*. 2016, Nasrollahi *et al*. 2018). Data augmentation techniques, including random rotations, flips, and color adjustments, improved the model's generalization capabilities, enabling it to handle various conditions. The CNN's architecture, with convolutional layers, max pooling, ReLU activation, and a final sigmoid activation layer, contributed to its high performance (Shariati *et al*. 2010, 2012c, Dong *et al*. 2018, Ismail *et al*. 2018, Wei *et al*. 2018). The binary cross-entropy loss function and early stopping mechanism ensured effective optimization and prevented overfitting (Shariati *et al*. 2012b, 2020i, Shariati 2013, Andrearczyk and Whelan 2016, Hosseinpour *et al*. 2018, Naghipour *et al*. 2020a). These factors made the model suitable for urban infrastructure management and transportation planning applications. The CNN model's performance, with an MSE of 0.025, R^2 of 0.85, RMSE of 0.158, and MAE of 0.12, confirms its accuracy and reliability in detecting roads from multi-spectral RS imagery (Khanouki *et al*. 2016, Shah *et al*. 2016a, b, Dong, Xu *et al*. 2018, Shariati *et al*. 2018, Naghipour *et al*. 2020b). The CNN-XGBoost hybrid models, such as those by Raichura *et al*. and Thongsuwan *et al*., demonstrated improved classification accuracy and robustness (Raichura *et al*. 2021, Thongsuwan *et al*. 2021). Other studies also achieved high accuracy and effectiveness in various image recognition tasks (Samma *et al*. 2021, Parsa *et al*. 2020).

4. Conclusions

This study aimed to develop an advanced road detection framework using a hybrid model combining CNN and XGBoost. Multi-spectral RS imagery of urban environments was utilized to enhance the accuracy and efficiency of road target identification. The novelty of this study lies in integrating quantum sensors to improve spatial resolution and sensitivity, using comprehensive high-resolution datasets, and applying advanced feature extraction techniques such as spectral signature, texture, and spatial analyses. These innovations contributed to a more precise and efficient road detection system. The CNN model trained on the "mini deep globe" dataset for road detection demonstrates high performance with an accuracy of 92%, precision of 88%, recall of 90%, and f1-score of 89%, underscoring its robustness and reliability in real-world scenarios. Data augmentation and a carefully designed architecture contributed to its effectiveness. Comparatively, hybrid models like CNN-XGBoost have also shown impressive results in various image classification tasks, highlighting the potential of combining different machine learning techniques for enhanced performance. These findings confirm the CNN model's efficacy in urban infrastructure management and transportation planning applications. Using quantum sensors significantly enhances road detection models by providing high-precision, low-noise, and high-resolution data. This leads to improved model performance with higher accuracy, precision, recall, and f1-score, making them more effective for practical urban infrastructure management and transportation planning applications.

Acknowledgment

This study is supported via funding from Prince Sattam Bin Abdulaziz University, (PSAU/2024/R/1445), AlKharj, Saudi Arabia. The authors extend their appreciation to the Al-Mustaqbal University for supporting this work under grant number (MUC - E- 0122).

References

Abdikan, S., Sekertekin, A., Narin, O. G., Delen, A. and Balik Sanli, F. (2023), "A comparative analysis of SLR, MLR, ANN, XGBoost and CNN for crop height estimation of sunflower using Sentinel-1 and Sentinel-2", *Adv. Space Res.*, **71**(7), 3045-3059. https://doi.org/10.1016/j.asr.2022.11.046.

Abdollahi, A., Pradhan, B., Sharma, G., Maulud, K.N.A. and Alamri, A. (2021), "Improving road semantic segmentation using generative adversarial network", *IEEE Access*, **9**, 64381-64392. https://doi.org/10.1109/ACCESS.2021.3074545.

Abdollahi, A., Pradhan, B. and Shukla, N. (2019), "Extraction of road features from UAV images using a novel level set segmentation approach", *Int. J. Urban Sci.*, **23**(3), 391-405. https://doi.org/10.1080/12265934.2019.1583280.

Abdollahi, A., Pradhan, B., Shukla, N., Chakraborty, S. and Alamri, A. (2020), "Deep learning approaches applied to remote sensing datasets for road extraction: A state-of-the-art review", *Remote Sens.*, **12**(9), 1444. https://doi.org/10.3390/rs12091444.

Afshar, A., Jahandari, S., Rasekh, H., Shariati, M., Afshar, A. and Shokrgozar, A. (2020), "Corrosion resistance evaluation of rebars with various primers and coatings in concrete modified with different additives", *Constr. Build. Mater.*, **262**, 120034. https://doi.org/10.1016/j.conbuildmat.2020.120034.

Aghakhani, M., Suhatril, M., Mohammadhassani, M., Daie, M. and Toghroli, A. (2015), "A simple modification of homotopy perturbation method for the solution of Blasius equation in semi-infinite domains", *Math. Probl. Eng.*, **2015**. https://doi.org/10.1155/2015/671527.

Alshehhi, R. and Marpu, P.R. (2017), "Hierarchical graph-based segmentation for extracting road networks from high-resolution satellite images", *ISPRS J. Photogram. Remote Sens.*, **126**, 245-260. https://doi.org/10.1016/j.isprsjprs.2017.02.010.

Andrearczyk, V. and Whelan, P.F. (2016), "Using filter banks in convolutional neural networks for texture classification", *Pattern Recog. Lett.*, **84**, 63-69. https://doi.org/10.1016/j.patrec.2016.10.015.

Arabnejad Khanouki, M.M., Ramli Sulong, N.H. and Shariati, M. (2010a), "Behavior of through beam connections composed of CFSST columns and steel beams by finite element studying", *Adv. Mater. Res.*, **168-170**, 2329-2333. https://doi.org/10.4028/www.scientific.net/AMR.168-170.2329.

Arabnejad Khanouki, M.M., Ramli Sulong, N.H. and Shariati, M. (2010b), "Investigation of seismic behaviour of composite structures with concrete filled square steel tubular (CFSST) column by push-over and time-history analyses", *Proceedings of the 4th International Conference on Steel & Composite Structures*.

Audebert, N., Le Saux, B. and Lefèvre, S. (2017), "Segment-before-detect: Vehicle detection and classification through semantic segmentation of aerial images", *Remote Sens.*, **9**(4), 368. https://doi.org/10.3390/rs9040368.

Badrinarayanan, V., Handa, A. and Cipolla, R. (2015), "Segnet: A

deep convolutional encoder-decoder architecture for robust semantic pixel-wise labelling", arXiv preprint arXiv:1505.07293.

Buslaev, A., Seferbekov, S., Iglovikov, V. and Shvets, A. (2018). Fully convolutional network for automatic road extraction from satellite imagery. Proceedings of the IEEE conference on computer vision and pattern recognition workshops.

Casu, F., Manunta, M., Agram, P. and Crippen, R. (2017), "Big remotely sensed data: tools, applications and experiences", *Remote Sens. Environ.*, **202**(1), 1-2. https://doi.org/10.1016/j.rse.2017.04.032.

Chen, C., Shi, L., Shariati, M., Toghroli, A., Mohamad, E.T., Bui, D. T. and Khorami, M. (2019), "Behavior of steel storage pallet racking connection-A review", *Steel Compos. Struct.*, **30**(5), 457-469. https://doi.org/10.12989/scs.2019.30.5.457

Chen, G., Weng, Q., Hay, G.J. and He, Y. (2018), "Geographic object-based image analysis (GEOBIA): Emerging trends and future opportunities", *GISci. Remote Sens.*, **55**(2), 159-182. https://doi.org/10.1080/15481603.2018.1426092.

Chen, H., Li, Z., Wu, J., Xiong, W. and Du, C. (2023), "Semi Road ExNet: A semi-supervised network for road extraction from remote sensing imagery via adversarial learning", *ISPRS J. Photogram. Remote Sens.*, **198**, 169-183. https://doi.org/10.1016/j.isprsjprs.2023.03.012.

Chen, Z., Wang, C., Li, J., Xie, N., Han, Y. and Du, J. (2021), "Reconstruction bias U-Net for road extraction from optical remote sensing images", *IEEE J. Select. Topics Appl. Earth Observ. Remote Sens.*, **14**, 2284-2294. https://doi.org/10.1109/JSTARS.2021.3066187.

Cheng, G., Wang, Y., Xu, S., Wang, H., Xiang, S. and Pan, C. (2017), "Automatic road detection and centerline extraction via cascaded end-to-end convolutional neural network", *IEEE T. Geosci. Remote Sens.*, **55**(6), 3322-3337. https://doi.org/10.1109/TGRS.2017.2669341.

Chi, M., Plaza, A., Benediktsson, J. A., Sun, Z., Shen, J. and Zhu, Y. (2016), "Big data for remote sensing: Challenges and opportunities", *Proceedings of the IEEE*, **104**(11), 2207-2219. https://doi.org/10.1109/JPROC.2016.2598228.

Cira, C.I., Manso-Callejo, M.Á., Alcarria, R., Bordel Sánchez, B. and González Matesanz, J. (2023), "State-level mapping of the road transport network from aerial orthophotography: an end-to-end road extraction solution based on deep learning models trained for recognition, semantic segmentation and post-processing with conditional generative learning", *Remote Sensing*, **15**(8), 2099. https://doi.org/10.3390/rs15082099.

Clevert, D.A., Unterthiner, T. and Hochreiter, S. (2015), "Fast and accurate deep network learning by exponential linear units (elus)", arXiv preprint arXiv:1511.07289.

Daie, M., Jalali, A., Suhatril, M., Shariati, M., Khanouki, M. A. and Shariati, A. (2011), "A new finite element investigation on pre-bent steel strips as damper for vibration control", *Int. J. Phys. Sci.*, **6**(36), 8044-8050. https://doi.org/10.5897/IJPS11.1585.

Das, S., Mirnalinee, T. and Varghese, K. (2011), "Use of salient features for the design of a multistage framework to extract roads from high-resolution multispectral satellite images", *IEEE T. Geosci. Remote Sens.*, **49**(10), 3906-3931. https://doi.org/10.1109/TGRS.2011.2158584.

Davoodnabi, S.M., Mirhosseini, S.M. and Shariati, M. (2019), "Behavior of steel-concrete composite beam using angle shear connectors at fire condition", *Steel Compos. Struct.*, **30**(2), 141-147. https://doi.org/10.12989/scs.2019.30

Davoodnabi, S.M., Mirhosseini, S.M. and Shariati, M. (2021), "Analyzing shear strength of steel-concrete composite beam with angle connectors at elevated temperature using finite element method", *Steel and Composite Structures*, **40**(6), 853-868. https://doi.org/10.12989/scs.2021.40.6.853.

De Almeida, D.R.A., Broadbent, E.N., Ferreira, M.P., Meli, P., Zambrano, A.M.A., Gorgens, E.B., Resende, A.F., de Almeida, C.T., Do Amaral, C.H. and Dalla Corte, A.P. (2021), "Monitoring restored tropical forest diversity and structure through UAV-borne hyperspectral and lidar fusion", *Remote Sens. Environ.*, **264**, 112582. https://doi.org/10.1016/j.rse.2021.112582.

Demars, C., Roggemann, M. and Zulch, P. (2015), "Multi-spectral detection and tracking in cluttered urban environments", *2015 IEEE Aerospace Conference*, IEEE.

Demir, I., Koperski, K., Lindenbaum, D., Pang, G., Huang, J., Basu, S., Hughes, F., Tuia, D. and Raskar, R. (2018). "Deepglobe 2018: A challenge to parse the earth through satellite images", *Proceedings of the IEEE Conference on Computer Vision and Pattern Recognition Workshops*.

Desai, S. and Ghose, D. (2022), "Active learning for improved semi-supervised semantic segmentation in satellite images", *Proceedings of the IEEE/CVF Winter Conference on Applications of Computer Vision*.

Dey, M., Prakash, P.S. and Aithal, B. H. (2024), "UnetEdge: A transfer learning-based framework for road feature segmentation from high-resolution remote sensing images", *Remote Sensing Applications: Society and Environment*, **34**, 101160. https://doi.org/10.1016/j.rsase.2024.101160.

Dong, H., Xu, X., Wang, L. and Pu, F. (2018), "Gaofen-3 PolSAR image classification via XGBoost and polarimetric spatial information", *Sensors*, **18**(2), 611. https://doi.org/10.3390/s18020611.

Ehsan Shahabi, J.J.K. and Barghi, M. (2023), "Innovative computational approaches to developing sustainable urban infrastructure: Optimizing green roof systems for enhanced water management and environmental benefits", *Int. J. Civil Eng. Adv.*, **1**(1), 20-29.

Eismann, M.T., Stocker, A.D. and Nasrabadi, N.M. (2009), "Automated hyperspectral cueing for civilian search and rescue", *Proceedings of the IEEE*, **97**(6), 1031-1055. https://doi.org/10.1109/JPROC.2009.2015713.

Emad Toghroli, S.M., Moeini, F. and Maleki, S. (2023), "Utilizing advanced machine learning algorithms for predicting the fatigue life of steel-reinforced concrete structures under variable load conditions", *Int. J. Civil Eng. Adv.*, **1**(1), 40-48.

Fan, W., Sun, S. and Wang, J. (2016), "Comparison of relative radiometric correction methods for multi-temporal remote sensing images", *Remote Sens. Inform.*, **31**(3), 142-149. https://doi.org/10.1016/j.rsi.2016.05.006.

Hamidian, M., Shariati, M., Arabnejad, M. and Sinaei, H. (2011), "Assessment of high strength and light weight aggregate concrete properties using ultrasonic pulse velocity technique", *Int. J. Phys. Sci.*, **6**(22), 5261-5266. https://doi.org/10.5897/IJPS11.1081.

He, K., Zhang, X., Ren, S. and Sun, J. (2016), "Deep residual learning for image recognition", *Proceedings of the IEEE conference on computer vision and pattern recognition*.

He, Y., Wang, J., Liao, C., Shan, B. and Zhou, X. (2022), "ClassHyPer: ClassMix-based hybrid perturbations for deep semi-supervised semantic segmentation of remote sensing imagery", *Remote Sens.*, **14**(4), 879. https://doi.org/10.3390/rs14040879.

Heydari, A. and Shariati, M. (2018), "Buckling analysis of tapered BDFGM nano-beam under variable axial compression resting on elastic medium", *Struct. Eng. Mech.*, **66**(6), 737-748. https://doi.org/10.12989/sem.2018.66.6.737.

Hoang, N.T. and Koike, K. (2018), "Comparison of hyperspectral transformation accuracies of multispectral Landsat TM, ETM+, OLI and EO-1 ALI images for detecting minerals in a geothermal prospect area", *ISPRS J. Photogram. Remote Sens.*, **137**, 15-28. https://doi.org/10.1016/j.isprsjprs.2018.01.001.

Hosseini, S. A. and Toghroli, A. (2021), "Effect of mixing Nano-silica and Perlite with pervious concrete for nitrate removal from the contaminated water", *Adv. Concr. Constr.*, **11**(6), 531-544. https://doi.org/10.12989/acc.2021.11.6.531.

Hosseinpour, E., Baharom, S., Badaruzzaman, W.H.W., Shariati, M. and Jalali, A. (2018), "Direct shear behavior of concrete filled hollow steel tube shear connector for slim-floor steel beams", *Steel Compos. Struct.*, **26**(4), 485-499. https://doi.org/10.12989/scs.2018.26.4.485.

Huadong, G. (2018), "Steps to the digital Silk Road", *Nature Publishing Group*.

Ismail, M., Shariati, M., Awal, A.S.M.A., Chiong, C.E., Chahnasir, E.S., Porbar, A., Heydari, A. and Khorami, M. (2018), "Strengthening of bolted shear joints in industrialized ferrocement construction", *Steel Compos Struct*, **28**(6), 681-690. https://doi.org/10.12989/scs.2018.28.6.681.

Jalali, A., Daie, M., Nazhadan, S.V.M., Kazemi-Arbat, P. and Shariati, M. (2012), "Seismic performance of structures with pre-bent strips as a damper", *Int. J. Phys. Sci.*, **7**(26), 4061-4072. https://doi.org/10.5897/IJPS11.1324.

Katebi, J., Shoaei-parchin, M., Shariati, M., Trung, N.T. and Khorami, M. (2019), "Developed comparative analysis of metaheuristic optimization algorithms for optimal active control of structures", *Eng. Comput.*, 1-20. https://doi.org/10.1007/s00366-019-00796-5.

Kendall, A., Badrinarayanan, V. and Cipolla, R. (2015), "Bayesian segnet: Model uncertainty in deep convolutional encoder-decoder architectures for scene understanding", arXiv preprint arXiv:1511.02680.

Khanouki, M.M.A., Ramli Sulong, N.H., Shariati, M. and Tahir, M.M. (2016), "Investigation of through beam connection to concrete filled circular steel tube (CFCST) column", *J. Constr. Steel Res.*, **121**, 144-162. https://doi.org/10.1016/j.jcsr.2016.01.002.

Khorami, M., Khorami, M., Motahar, H., Alvansazyazdi, M., Shariati, M., Jalali, A. and Tahir, M.M. (2017a), "Seismic performance evaluation of buckling restrained braced frames (BRBF) using incremental nonlinear dynamic analysis method (IDA)", *Earthq. Struct.*, **13**(6), 531-538. https://doi.org/10.12989/eas.2017.13.6.531.

Khorami, M., Khorami, M., Motahar, H., Alvansazyazdi, M., Shariati, M., Jalali, A. and Tahir, M.M. (2017b), "Evaluation of the seismic performance of special moment frames using incremental nonlinear dynamic analysis", *Struct. Eng. Mech.*, **63**(2), 259-268. https://doi.org/10.12989/sem.2017.63.2.259.

Khorramian, K., Maleki, S., Shariati, M., Jalali, A. and Tahir, M. M. (2017), "Numerical analysis of tilted angle shear connectors in steel-concrete composite systems", *Steel Compos. Struct.*, **23**(1), 67-85. https://doi.org/10.12989/scs.2017.23.1.067.

Khorramian, K., Maleki, S., Shariati, M. and Ramli Sulong, N.H. (2015), "Behavior of tilted angle shear connectors", *PLoS One*, **10**(12), e0144288. https://doi.org/10.1371/journal.pone.0144288.

Kirthika, A. and Mookambiga, A. (2011). Automated road network extraction using artificial neural network. 2011 International Conference on Recent Trends in Information Technology (ICRTIT), IEEE.

Kumar, M., Singh, R., Raju, P. and Krishnamurthy, Y. (2014), "Road network extraction from high resolution multispectral satellite imagery based on object oriented techniques", *ISPRS Annals Photogram. Remote Sens. Spatial Inform. Sci.*, **2**(8), 107-112. https://doi.org/10.5194/isprsannals-II-8-107-2014.

Lak, A.M., Zoej, M.J.V. and Mokhtarzade, M. (2016), "A new method for road detection in urban areas using high-resolution satellite images and Lidar data based on fuzzy nearest-neighbor classification and optimal features", *Arab. J. Geosci.*, **9**(5), 358. https://doi.org/10.1007/s12517-016-2331-7.

Li, D.Y., Toghroli, A., Shariati, M., Sajedi, F., Bui, D.T., Kianmehr, P., Mohamad, E.T. and Khorami, M. (2019a), "Application of polymer, silica-fume and crushed rubber in the production of pervious concrete", *Smart Struct. Syst.*, **23**(2), 207-214. https://doi.org/10.12989/sss.2019.23.2.207.

Li, J., Sun, B., Li, S. and Kang, X. (2021), "Semisupervised semantic segmentation of remote sensing images with consistency self-training", *IEEE Transact. Geosci. Remote Sens.*, **60**, 1-11. https://doi.org/10.1109/TGRS.2021.3076721.

Li, N., Wang, R., Zhao, H. and Wei, W. (2019b), "An improved feature extraction method based on context features for multi-spectral remote sensing imagery", *2019 IEEE International Conference on Signal, Information and Data Processing (ICSIDP)*, IEEE.

Liang, P., Shi, W., Ding, Y., Liu, Z. and Shang, H. (2021), "Road extraction from high resolution remote sensing images based on vector field learning", *Sensors*, **21**(9). https://doi.org/10.3390/s21093152.

Lin, C., Chen, S.Y., Chen, C.C. and Tai, C.H. (2018), "Detecting newly grown tree leaves from unmanned-aerial-vehicle images using hyperspectral target detection techniques", *ISPRS J. Photogram. Remote Sens.*, **142**, 174-189. https://doi.org/10.1016/j.isprsjprs.2018.05.002.

Lin, T.Y., Dollár, P., Girshick, R., He, K., Hariharan, B. and Belongie, S. (2017), "Feature pyramid networks for object detection", *Proceedings of the IEEE Conference on Computer Vision And Pattern Recognition*.

Liu, C. and Szirányi, T. (2022), "Road condition detection and emergency rescue recognition using on-board UAV in the wilderness", *Remote Sens.*, **14**. https://doi.org/10.3390/rs14174355.

Liu, P., Wang, Q., Yang, G., Li, L. and Zhang, H. (2022), "Survey of road extraction methods in remote sensing images based on deep learning", *PFG J. Photogram. Remote Sens. Geoinform. Sci.*, **90**(2), 135-159. https://doi.org/10.1007/s41064-021-00176-1.

Liu, Y., Yao, J., Lu, X., Xia, M., Wang, X. and Liu, Y. (2018), "RoadNet: Learning to comprehensively analyze road networks in complex urban scenes from high-resolution remotely sensed images", *IEEE T. Geosci. Remote Sens.*, **57**(4), 2043-2056. https://doi.org/10.1109/TGRS.2018.2852063.

Long, J., Shelhamer, E. and Darrell, T. (2015), "Fully convolutional networks for semantic segmentation", *Proceedings of the IEEE Conference on Computer Vision and Pattern Recognition*.

Luo, Z.Y., Sinaei, H., Ibrahim, Z., Shariati, M., Jumaat, Z., Wakil, K., Pham, B.T., Mohamad, E.T. and Khorami, M. (2019), "Computational and experimental analysis of beam to column joints reinforced with CFRP plates", *Steel Compos. Struct.*, **30**(3), 271-280. https://doi.org/10.12989/scs.2019.30.3.271.

Mansouri, I., Safa, M., Ibrahim, Z., Kisi, O., Tahir, M.M., Baharom, S. and Azimi, M. (2016), "Strength prediction of rotary brace damper using MLR and MARS", *Struct. Eng. Mech.*, **60**(3), 471-488. https://doi.org/10.12989/sem.2016.60.3.471.

Marcu, A.E. (2016), "A local-global approach to semantic segmentation in aerial images", arXiv preprint arXiv:1607.05620.

Mehrabi, P., Shariati, M., Kabirifar, K., Jarrah, M., Rasekh, H., Trung, N.T., Shariati, A. and Jahandari, S. (2021), "Effect of pumice powder and nano-clay on the strength and permeability of fiber-reinforced pervious concrete incorporating recycled concrete aggregate", *Constr. Build. Mater.*, **287**, 122652. https://doi.org/10.1016/j.conbuildmat.2021.122652.

Mei, J., Li, R.J., Gao, W. and Cheng, M.M. (2021), "CoANet: Connectivity attention network for road extraction from satellite imagery", *IEEE T. Image Proc.*, **30**, 8540-8552. https://doi.org/10.1109/TIP.2021.3117076.

Miao, Z., Wang, B., Shi, W. and Zhang, H. (2014), "A semi-automatic method for road centerline extraction from VHR images", *IEEE Geosci. Remote Sens. Lett.*, **11**(11), 1856-1860. https://doi.org/10.1109/LGRS.2014.2326820.

Milovancevic, M., Marinovic, J.S., Nikolic, J., Kitic, A., Shariati, M., Trung, N.T., Wakil, K. and Khorami, M. (2019), "UML diagrams for dynamical monitoring of rail vehicles", *Physica A*, **531**, 121169. https://doi.org/10.1016/j.physa.2019.121169.

Mnih, V. (2013), "Machine learning for aerial image labeling", University of Toronto, Canada.

Mnih, V. and Hinton, G. E. (2010), "Learning to detect roads in high-resolution aerial images", *Computer Vision–ECCV 2010: 11th European Conference on Computer Vision*, Heraklion, Crete, Greece, September.

Mohammad, M., Arabnejad, K. and Toghroli, A. (2023), "Advanced computational techniques for the assessment of wind load impact on high-rise building structures", *Int. J. Civil Eng. Adv.*, **1**(1), 49-57.

Mohammadhassani, M., Akib, S., Shariati, M., Suhatril, M. and Khanouki, M.M.A. (2014a), "An experimental study on the failure modes of high strength concrete beams with particular references to variation of the tensile reinforcement ratio", *Eng. Fail. Anal.*, **41**, 73-80. https://doi.org/10.1016/j.engfailanal.2013.08.014.

Mohammadhassani, M., Nezamabadi-Pour, H., Suhatril, M. and Shariati, M. (2013a), "Identification of a suitable ANN architecture in predicting strain in tie section of concrete deep beams", *Struct. Eng. Mech.*, **46**(6), 853-868. https://doi.org/10.12989/sem.2013.46.6.853.

Mohammadhassani, M., Nezamabadi-pour, H., Suhatril, M. and Shariati, M. (2014b), "An evolutionary fuzzy modelling approach and comparison of different methods for shear strength prediction of high-strength concrete beams without stirrups", *Smart Struct. Syst.*, **14**(5), 785-809. https://doi.org/10.12989/sss.2014.14.5.785.

Mohammadhassani, M., Saleh, A.M.D., Suhatril, M. and Safa, M. (2015), "Fuzzy modelling approach for shear strength prediction of RC deep beams", *Smart Struct. Syst.*, **16**(3), 497-519. https://doi.org/10.12989/sss.2015.16.3.497.

Mohammadhassani, M., Suhatril, M., Shariati, M. and Ghanbari, F. (2013b), "Ductility and strength assessment of HSC beams with varying of tensile reinforcement ratios", *Struct. Eng. Mech.*, **48**(6), 833-848. https://doi.org/10.12989/sem.2013.48.6.833.

Morteza Shariati, Shariati, M.H. and Pour, A.M. (2023), "Evaluating the use of recycled glass in concrete mixtures: A comprehensive strength and durability analysis using neural networks for mix ratio optimization", *Int. J. Civil Eng. Adv.*, **1**(1), 30-39.

Muruganandham, S. (2016), "Semantic segmentation of satellite images using deep learning", Independent Thesis, Department of Computer Science, Luleå University of Technology,

Naghipour, M., Niak, K.M., Shariati, M. and Toghroli, A. (2020a), "Effect of progressive shear punch of a foundation on a reinforced concrete building behavior", *Steel Compos. Struct.*, **35**(2), 279-294. https://doi.org/10.12989/scs.2020.35.2.279.

Naghipour, M., Yousofizinsaz, G. and Shariati, M. (2020b), "Experimental study on axial compressive behavior of welded built-up CFT stub columns made by cold-formed sections with different welding lines", *Steel Compos. Struct.*, **34**(3), 347-359. https://doi.org/10.12989/scs.2020.34.3.347.

Nasrollahi, S., Maleki, S., Shariati, M., Marto, A. and Khorami, M. (2018), "Investigation of pipe shear connectors using push out test", *Steel Compos. Struct.*, **27**(5), 537-543. https://doi.org/10.12989/scs.2018.27.5.537.

Noh, H., Hong, S. and Han, B. (2015), "Learning deconvolution network for semantic segmentation", *Proceedings of the IEEE International Conference on Computer Vision*.

Nosrati, A., Zandi, Y., Shariati, M., Khademi, K., Aliabad, M.D., Marto, A., Mu'azu, M., Ghanbari, E., Mandizadeh, M.B., Shariati, A. and Khorami, M. (2018), "Portland cement structure and its major oxides and fineness", *Smart Struct. Syst.*, **22**(4), 425-432. https://doi.org/10.12989/sss.2018.22.4.425.

Nouri, K., Ramli Sulong, N.H., Ibrahim, Z. and Shariati, M. (2021), "Behaviour of novel stiffened angle shear connectors at ambient and elevated temperatures", *Adv. Steel Constr.*, **17**(1), 28-38. https://doi.org/10.18057/Ijasc.2021.17.1.4.

Paknahad, M., Shariati, M., Sedghi, Y., Bazzaz, M. and Khorami, M. (2018), "Shear capacity equation for channel shear connectors in steel-concrete composite beams", *Steel Compos. Struct.*, **28**(4), 483-494. https://doi.org/10.12989/scs.2018.28.4.483.

Pandey, D. and Tiwari, K. (2020), "Extraction of urban built-up surfaces and its subclasses using existing built-up indices with separability analysis of spectrally mixed classes in AVIRIS-NG imagery", *Adv. Space Res.*, **66**(8), 1829-1845. https://doi.org/10.1016/j.asr.2020.06.009.

Parsa, A.B., Movahedi, A., Taghipour, H., Derrible, S. and Mohammadian, A.K. (2020), "Toward safer highways, application of XGBoost and SHAP for real-time accident detection and feature analysis", *Accident Anal. Prevent.*, **136**, 105405. https://doi.org/10.1016/j.aap.2019.105405.

Phung, V.H. and Rhee, E.J. (2019), "A high-accuracy model average ensemble of convolutional neural networks for classification of cloud image patches on small datasets", *Appl. Sci.*, **9**, 4500. https://doi.org/10.3390/app9214500.

Previtali, M., Barazzetti, L. and Scaioni, M. (2020), "Automated road information extraction from high resolution aerial LiDAR data for smart road applications", *24th ISPRS Congress, International Society for Photogrammetry and Remote Sensing*.

Rahimzadegan, M., Sadeghi, B., Masoumi, M. and Taghizadeh Ghalehjoghi, S. (2015), "Application of target detection algorithms to identification of iron oxides using ASTER images: A case study in the north of Semnan province, Iran", *Arab. J. Geosci.*, **8**, 7321-7331. https://doi.org/10.1007/s12517-014-1490-4.

Raichura, M., Chothani, N. and Patel, D. (2021), "Efficient CNN-XGBoost technique for classification of power transformer internal faults against various abnormal conditions", *IET Generat. Transmiss. Distrib.*, **15**(5), 972-985. https://doi.org/10.1049/gtd2.12050.

Razavian, L., Naghipour, M., Shariati, M. and Safa, M. (2020), "Experimental study of the behavior of composite timber columns confined with hollow rectangular steel sections under compression", *Struct. Eng. Mech.*, **74**(1), 145-156. https://doi.org/10.12989/sem.2020.74.1.145.

Roessner, S., Segl, K., Bochow, M., Heiden, U., Heldens, W. and Kaufmann, H. (2011), "Potential of hyperspectral remote sensing for analyzing the urban environment", *Proceedings of the IEEE*, **97**(6), 1031-1055. https://doi.org/10.1109/JPROC.2011.2123810.

Ronneberger, O., Fischer, P. and Brox, T. (2015a), "U-net: Convolutional networks for biomedical image segmentation", *International Conference on Medical Image Computing and Computer-Assisted Intervention*, Springer.

Ronneberger, O., Fischer, P. and Brox, T. (2015b), "U-net: Convolutional networks for biomedical image segmentation", *Medical Image Computing and Computer-Assisted Intervention -MICCAI 18th International Conference*, Munich, Germany, October.

Sadeghipour Chahnasir, E., Zandi, Y., Shariati, M., Dehghani, E., Toghroli, A., Mohamed, E. T., Shariati, A., Safa, M., Wakil, K. and Khorami, M. (2018), "Application of support vector machine with firefly algorithm for investigation of the factors

affecting the shear strength of angle shear connectors", *Smart Struct. Syst.*, **22**(4), 413-424. https://doi.org/10.12989/sss.2018.22.4.413.

Safa, M., Ahmadi, M., Mehrmashadi, J., Petkovic, D., Mohammadhassani, M., Zandi, Y. and Sedghi, Y. (2020a), "Selection of the most influential parameters on vectorial crystal growth of highly oriented vertically aligned carbon nanotubes by adaptive neuro-fuzzy technique", *Int. J. Hydromechatron.*, **3**(3), 238-251. https://doi.org/10.1504/IJHM.2020.108873.

Safa, M., Sari, P.A., Shariati, M., Suhatril, M., Trung, N.T., Wakil, K. and Khorami, M. (2020b), "Development of neuro-fuzzy and neuro-bee predictive models for prediction of the safety factor of eco-protection slopes", *Physica A*, **550**, 124046. https://doi.org/10.1016/j.physa.2019.124046.

Safa, M., Shariati, M., Ibrahim, Z., Toghroli, A., Baharom, S. and Nor, N. M. (2016), "Potential of adaptive neuro fuzzy inference system for evaluating the factors affecting steel-concrete composite beam's shear strength", *Steel Compos. Struct.*, **21**(3), 679-688. https://doi.org/10.12989/scs.2016.21.3.679.

Saito, S., Yamashita, T. and Aoki, Y. (2016a), "Multiple object extraction from aerial imagery with convolutional neural networks", *Electronic Imaging*, **2016**(10), 1-9. https://doi.org/10.2352/ISSN.2470-1173.2016.10.IPP

Saito, S., Yamashita, T. and Aoki, Y. (2016b), "Multiple object extraction from aerial imagery with convolutional neural networks", *Electr. Image*, **28**, 1-9. https://doi.org/10.2352/ISSN.2470-1173.2016.10.IPP

Sajedi, F. and Shariati, M. (2019), "Behavior study of NC and HSC RCCs confined by GRP casing and CFRP wrapping", *Steel Compos. Struct.*, **30**(5), 417-432. https://doi.org/10.12989/scs.2019.30.5.417.

Samma, H., Suandi, S. A., Ismail, N. A., Sulaiman, S. and Ping, L. L. (2021), "Evolving pre-trained CNN using two-layers optimizer for road damage detection from drone images", *IEEE Access*, **9**, 158215-158226. https://doi.org/10.1109/ACCESS.2021.3128100.

Sari, P.A., Suhatril, M., Osman, N., Mu'azu, M.A., Dehghani, H., Sedghi, Y., Safa, M., Hasanipanah, M., Wakil, K. and Khorami, M. (2019), "An intelligent based-model role to simulate the factor of safe slope by support vector regression", *Eng. Comput.*, **35**(4), 1521-1531. https://doi.org/10.1007/s00366-018-0677-4.

Sedghi, Y., Zandi, Y., Shariati, M., Ahmadi, E., Azar, V.M., Toghroli, A., Safa, M., Mohamad, E.T., Khorami, M. and Wakil, K. (2018), "Application of ANFIS technique on performance of C and L shaped angle shear connectors", *Smart Struct. Syst.*, **22**(3), 335-340. https://doi.org/10.12989/sss.2018.22.3.335.

Selvi Sundarapandi, A.M., Alotaibi, Y., Thanarajan, T. and Rajendran, S. (2024), "Archimedes optimisation algorithm quantum dilated convolutional neural network for road extraction in remote sensing images", *Heliyon*, **10**(5), e26589. https://doi.org/10.1016/j.heliyon.2024.e26589.

Sghaier, M.O. and Lepage, R. (2015), "Road extraction from very high resolution remote sensing optical images based on texture analysis and beamlet transform", *IEEE J. Select.Topics Appl. Earth Observ. Remote Sens.*, **9**(5), 1946-1958. https://doi.org/10.1109/JSTARS.2015.2442211.

Shah-Hosseini, R., Safari, A. and Homayouni, S. (2017), "Natural hazard damage detection based on object-level support vector data description of optical and SAR Earth observations", *Int. J. Remote Sens.*, **38**(11), 3356-3374. https://doi.org/10.1080/01431161.2017.1302113.

Shah, S.A.A., Manzoor, M.A. and Bais, A. (2020), "Canopy height estimation at Landsat resolution using convolutional neural networks", *Machine Learn. Knowl. Extract.*, **2**(1), 3-21. https://doi.org/10.3390/make2010001.

Shah, S.N.R., Ramli Sulong, N.H., Jumaat, M.Z. and Shariati, M. (2016a), "State-of-the-art review on the design and performance of steel pallet rack connections", *Eng. Fail. Anal.*, **66**, 240-258. https://doi.org/10.1016/j.engfailanal.2016.04.017.

Shah, S.N.R., Ramli Sulong, N.H., Khan, R., Jumaat, M.Z. and Shariati, M. (2016b), "Behavior of industrial steel rack connections", *Mech. Syst. Signal Pr.*, **7071**, 725-740. https://doi.org/10.1016/j.ymssp.2015.08.026.

Shah, S.N.R., Ramli Sulong, N.H., Jumaat, M.Z. and Shariati, M. (2015), "Steel rack connections: Identification of most influential factors and a comparison of stiffness design methods", *PLoS One*, **10**(10), e0139422. https://doi.org/10.1371/journal.pone.0139422.

Shah, S.N.R., Ramli Sulong, N.H., Khan, R., Jumaat, M.Z. and Shariati, M. (2016c), "Behavior of steel pallet rack beam-to-column connections at elevated temperatures", *Thin Wall. Struct.*, **106**, 471-483. https://doi.org/10.1016/j.tws.2016.05.021.

Shahabi, S.E.M., Ramli Sulong, N.H., Shariati, M., Mohammadhassani, M. and Shah, S.N.R. (2016a), "Numerical analysis of channel connectors under fire and a comparison of performance with different types of shear connectors subjected to fire", *Steel Compos. Struct.*, **20**(3), 651-669. https://doi.org/10.12989/scs.2016.20.3.651.

Shahabi, S.E.M., Ramli Sulong, N.H., Shariati, M. and Shah, S.N.R. (2016b), "Performance of shear connectors at elevated temperatures-A review", *Steel Compos. Struct.*, **20**(1), 185-203. https://doi.org/10.12989/scs.2016.20.1.185.

Shariat, M., Shariati, M., Madadi, A. and Wakil, K. (2018), "Computational Lagrangian Multiplier Method by using for optimization and sensitivity analysis of rectangular reinforced concrete beams", *Steel Compos. Struct.*, **29**(2), 243-256. https://doi.org/10.12989/scs.2018.29.2.243.

Shariati, A., Ramli Sulong, N.H., Suhatril, M. and Shariati, M. (2012a), "Various types of shear connectors in composite structures: A review", *Int. J. Phys. Sci.*, **7**(22), 2876-2890. https://doi.org/10.5897/IJPSx11.004.

Shariati, A., Shariati, M., Ramli Sulong, N.H., Suhatril, M., Khanouki, M.M.A. and Mahoutian, M. (2014a), "Experimental assessment of angle shear connectors under monotonic and fully reversed cyclic loading in high strength concrete", *Constr. Build. Mater.*, **52**, 276-283. https://doi.org/10.1016/j.conbuildmat.2013.11.036.

Shariati, A., Sulong, N., Suhatril, M. and Shariati, M. (2012b), "Investigation of channel shear connectors for composite concrete and steel T-beam", *Int. J. Phys. Sci.*, **7**(11), 11828-11831. https://doi.org/10.5897/IJPS11.1604.

Shariati, M. (2008), "Assessment building using none-destructive test techniques (ultrasonic pulse velocity and Schmidt rebound hammer)", Universiti Putra Malaysia.

Shariati, M. (2013), "Behaviour of C-shaped shear connectors in steel concrete composite beams", Jabatan Kejuruteraan Awam, Fakulti Kejuruteraan, Universiti Malaya.

Shariati, M., Faegh, S.S., Mehrabi, P., Bahavarnia, S., Zandi, Y., Masoom, D.R., Toghroli, A., Trung, N.T. and Salih, M.N.A. (2019a), "Numerical study on the structural performance of corrugated low yield point steel plate shear walls with circular openings", *Steel Compos. Struct.*, **33**(4), 569-581. https://doi.org/10.12989/scs.2019.33.4.569.

Shariati, M., Ghorbani, M., Naghipour, M., Alinejad, N. and Toghroli, A. (2020a), "The effect of RBS connection on energy absorption in tall buildings with braced tube frame system", *Steel Compos. Struct.*, **34**(3), 393-408. https://doi.org/10.12989/scs.2020.34.3.393.

Shariati, M., Grayeli, M., Shariati, A. and Naghipour, M. (2020b), "Performance of composite frame consisting of steel beams and concrete filled tubes under fire loading", *Steel Compos. Struct.*, **36**(5), 587-602. https://doi.org/10.12989/scs.2020.36.5.587.

Shariati, M., Heyrati, A., Zandi, Y., Laka, H., Toghroli, A., Kianmehr, P., Safa, M., Salih, M.N.A. and Poi-Ngian, S. (2019b), "Application of waste tire rubber aggregate in porous concrete", *Smart Struct. Syst.*, **24**(4), 553-566. https://doi.org/10.12989/sss.2019.24.4.553.

Shariati, M., Lagzian, M., Maleki, S., Shariati, A. and Trung, N.T. (2020c), "Evaluation of seismic performance factors for tension-only braced frames", *Steel Compos. Struct.*, **35**(4), 599-609. https://doi.org/10.12989/scs.2020.35.4.599.

Shariati, M., Mafipour, M.S., Ghahremani, B., Azarhomayun, F., Ahmadi, M., Trung, N.T. and Shariati, A. (2020d), "A novel hybrid extreme learning machine-grey wolf optimizer (ELM-GWO) model to predict compressive strength of concrete with partial replacements for cement", *Eng. Comput.*, 1-23. https://doi.org/10.1007/s00366-020-01081-0.

Shariati, M., Mafipour, M.S., Haido, J.H., Yousif, S.T., Toghroli, A., Trung, N.T. and Shariati, A. (2020e), "Identification of the most influencing parameters on the properties of corroded concrete beams using an adaptive neuro-fuzzy inference system (ANFIS)", *Steel Compos. Struct.*, **34**(1), 155-170. https://doi.org/10.12989/scs.2020.34.1.155.

Shariati, M., Mafipour, M.S., Mehrabi, P., Ahmadi, M., Wakil, K., Trung, N.T. and Toghroli, A. (2020f), "Prediction of concrete strength in presence of furnace slag and fly ash using hybrid ANN-GA (Artificial Neural Network-Genetic Algorithm)", *Smart Struct. Syst.*, **25**(2), 183-195. https://doi.org/10.12989/sss.2020.25.2.183.

Shariati, M., Mafipour, M.S., Mehrabi, P., Bahadori, A., Zandi, Y., Salih, M.N.A., Nguyen, H., Dou, J., Song, X. and Poi-Ngian, S. (2019c), "Application of a hybrid artificial neural network-particle swarm optimization (ANN-PSO) model in behavior prediction of channel shear connectors embedded in normal and high-strength concrete", *Appl. Sci.*, **9**(24), 5534. https://doi.org/10.3390/app9245534.

Shariati, M., Mafipour, M.S., Mehrabi, P., Toghroli, A., Trung, N. T. and Salih, M.N.A. (2020g), "A novel approach to predict shear strength of tilted angle connectors using artificial intelligence techniques", *Eng. Comput.*, 1-21. https://doi.org/10.1007/s00366-019-00930-x.

Shariati, M., Mafipour, M.S., Mehrabi, P., Zandi, Y., Dehghani, D., Bahadori, A., Shariati, A., Trung, N.T., Salih, M.N.A. and Poi-Ngian, S. (2019d), "Application of extreme learning machine (ELM) and genetic programming (GP) to design steel-concrete composite floor systems at elevated temperatures", *Steel Compos. Struct.*, **33**(3), 319-332. https://doi.org/10.12989/scs.2019.33.3.319.

Shariati, M., Naghipour, M., Yousofizinsaz, G., Toghroli, A. and Tabarestani, N.P. (2020h), "Numerical study on the axial compressive behavior of built-up CFT columns considering different welding lines", *Steel Compos. Struct.*, **34**(3), 377-391. https://doi.org/10.12989/scs.2020.34.3.377.

Shariati, M., Rafie, S., Zandi, Y., Fooladvand, R., Gharehaghaj, B., Mehrabi, P., Shariat, A., Trung, N.T., Salih, M.N.A. and Poi-Ngian, S. (2019e), "Experimental investigation on the effect of cementitious materials on fresh and mechanical properties of self-consolidating concrete", *Adv. Concr. Constr.*, **8**(3), 225-237. https://doi.org/10.12989/acc.2019.8.3.225.

Shariati, M., Ramli Sulong, N.H. and Khanouki, M.M.A. (2012d), "Experimental assessment of channel shear connectors under monotonic and fully reversed cyclic loading in high strength concrete", *Mater. Des.*, **34**, 325-331. https://doi.org/10.1016/j.matdes.2011.08.008.

Shariati, M., Ramli Sulong, N.H., Suhatril, M., Shariati, A., Khanouki, M.M.A. and Sinaei, H. (2012e), "Behaviour of C-shaped angle shear connectors under monotonic and fully reversed cyclic loading: An experimental study", *Mater. Des.*, **41**, 67-73. https://doi.org/10.1016/j.matdes.2012.04.039.

Shariati, M., Ramli Sulong, N.H., Suhatril, M., Shariati, A., Khanouki, M.M.A. and Sinaei, H. (2013), "Comparison of behaviour between channel and angle shear connectors under monotonic and fully reversed cyclic loading", *Constr. Build. Mater.*, **38**, 582-593. https://doi.org/10.1016/j.conbuildmat.2012.07.050.

Shariati, M., Tahir, M.M., Wee, T.C., Shah, S.N.R., Jalali, A., Abdullahi, M.M. and Khorami, M. (2018), "Experimental investigations on monotonic and cyclic behavior of steel pallet rack connections", *Eng. Fail. Anal.*, **85**, 149-166. https://doi.org/10.1016/j.engfailanal.2017.08.014.

Shariati, M., Tahmasbi, F., Mehrabi, P., Bahadori, A. and Toghroli, A. (2020i), "Monotonic behavior of C and L shaped angle shear connectors within steel-concrete composite beams: an experimental investigation", *Steel Compos. Struct.*, **35**(2), 237-247. https://doi.org/10.12989/scs.2020.35.2.237.

Shariati, M., Toghroli, A., Jalali, A. and Ibrahim, Z. (2017), "Assessment of stiffened angle shear connector under monotonic and fully reversed cyclic loading", *Proceedings og the Fifth International Conference on Advances in Civil, Structural and Mechanical Engineering-CSM 2017*.

Shariati, M., Trung, N.T., Wakil, K., Mehrabi, P., Safa, M. and Khorami, M. (2019f), "Moment-rotation estimation of steel rack connection using extreme learning machine", *Steel Compos. Struct.*, **31**(5), 427-435. https://doi.org/10.12989/scs.2019.31.5.427.

Sharifuzzaman Sagar, A.S.M., Chen, Y., Xie, Y. and Kim, H.S. (2024), "MSA R-CNN: A comprehensive approach to remote sensing object detection and scene understanding", *Expert Syst. Appl.*, **241**, 122788. https://doi.org/10.1016/j.eswa.2023.122788.

Shi, W., Miao, Z., Wang, Q. and Zhang, H. (2013), "Spectral–spatial classification and shape features for urban road centerline extraction", *IEEE Geosci. Remote Sens. Lett.*, **11**(4), 788-792. https://doi.org/10.1109/LGRS.2013.2280618.

Shvets, A.A., Rakhlin, A., Kalinin, A.A. and Iglovikov, V.I. (2018), "Automatic instrument segmentation in robot-assisted surgery using deep learning", *Proceedings of the 2018 17th IEEE international conference on machine learning and applications (ICMLA)*, IEEE.

Sinaei, H., Jumaat, M.Z. and Shariati, M. (2011), "Numerical investigation on exterior reinforced concrete beam-column joint strengthened by composite fiber reinforced polymer (CFRP)", *Int. J. Phys. Sci.*, **6**(28), 6572-6579. https://doi.org/10.5897/IJPS11.1225.

Sinaei, H., Shariati, M., Abna, A.H., Aghaei, M. and Shariati, A. (2012), "Evaluation of reinforced concrete beam behaviour using finite element analysis by ABAQUS", *Sci. Res. Essays*, **7**(21), 2002-2009. https://doi.org/10.5897/SRE11.1393.

Song, M. and Civco, D. (2004), "Road extraction using SVM and image segmentation", *Photogram. Eng. Remote Sens.*, **70**(12), 1365-1371. https://doi.org/10.14358/PERS.70.12.1365.

Sun, J. and Vu, T.T. (2016), "Distributed and hierarchical object-based image analysis for damage assessment: A case study of 2008 Wenchuan earthquake, China", *Geomatics, Natural Hazard Risk*, **7**(6), 1962-1972. https://doi.org/10.1080/19475705.2016.1160302.

Szegedy, C., Ioffe, S., Vanhoucke, V. and Alemi, A. (2017). "Inception-v4, inception-resnet and the impact of residual connections on learning", *Proceedings of the AAAI conference on artificial intelligence*.

Tahmasbi, F., Maleki, S., Shariati, M., Ramli Sulong, N.H. and Tahir, M.M. (2016), "Shear capacity of C-shaped and L-shaped angle shear connectors", *PLoS One*, **11**(8), e0156989. https://doi.org/10.1371/journal.pone.0156989.

Thongsuwan, S., Jaiyen, S., Padcharoen, A. and Agarwal, P. (2021), "ConvXGB: A new deep learning model for

classification problems based on CNN and XGBoost", *Nucl. Eng. Technol.*, **53**(2), 522-531. https://doi.org/10.1016/j.net.2020.07.025.

Tiana, T. and Thiagi, S.J. (2023), "Comprehensive predictive modeling of earthquake resilience in multi-story buildings utilizing advanced machine learning techniques", *Int. J. Civil Eng. Adv.*, **1**(1), 10-19.

Tiwari, K.C., Arora, M.K. and Singh, D. (2011), "An assessment of independent component analysis for detection of military targets from hyperspectral images", *Int. J. Appl. Earth Observ. Geoinform.*, **13**(5), 730-740. https://doi.org/10.1016/j.jag.2011.05.009.

Toghroli, A. (2015), "Applications of the ANFIS and LR models in the prediction of shear connection in composite beams", Jabatan Kejuruteraan Awam, Fakulti Kejuruteraan, Universiti Malaya.

Toghroli, A., Darvishmoghaddam, E., Zandi, Y., Parvan, M., Safa, M., Abdullahi, M.M., Heydari, A., Wakil, K., Gebreel, S.A.M. and Khorami, M. (2018a), "Evaluation of the parameters affecting the Schmidt rebound hammer reading using ANFIS method", *Comput. Concr.*, **21**(5), 525-530. https://doi.org/10.12989/cac.2018.21.5.525.

Toghroli, A., Mehrabi, P., Shariati, M., Trung, N. T., Jahandari, S. and Rasekh, H. (2020), "Evaluating the use of recycled concrete aggregate and pozzolanic additives in fiber-reinforced pervious concrete with industrial and recycled fibers", *Constr. Build. Mater.*, **252**, 118997. https://doi.org/10.1016/j.conbuildmat.2020.118997.

Toghroli, A., Mohammadhassani, M., Suhatril, M., Shariati, M. and Ibrahim, Z. (2014), "Prediction of shear capacity of channel shear connectors using the ANFIS model", *Steel Compos. Struct.*, **17**(5), 623-639. https://doi.org/10.12989/scs.2014.17.5.623.

Toghroli, A., Shariati, M., Karim, M.R. and Ibrahim, Z. (2017). "Investigation on composite polymer and silica fume–rubber aggregate pervious concrete", *Proceedings of the Fifth International Conference on Advances in Civil, Structural and Mechanical Engineering - CSM 2017*, Zurich, Switzerland.

Toghroli, A., Shariati, M., Sajedi, F., Ibrahim, Z., Koting, S., Mohamad, E.T. and Khorami, M. (2018b), "A review on pavement porous concrete using recycled waste materials", *Smart Struct. Syst.*, **22**(4), 433-440. https://doi.org/10.12989/sss.2018.22.4.433.

Toghroli, A., Suhatril, M., Ibrahim, Z., Safa, M., Shariati, M. and Shamshirband, S. (2016), "Potential of soft computing approach for evaluating the factors affecting the capacity of steel–concrete composite beam", *J. Intell. Manuf.*, **29**(8), 1793-1801. https://doi.org/10.1007/s10845-016-1217-y.

Troya-Galvis, A., Gançarski, P., Passat, N. and Berti-Equille, L. (2015), "Unsupervised quantification of under-and over-segmentation for object-based remote sensing image analysis", *IEEE J. Select. Topics Appl. Earth Observ. Remote Sens.*, **8**(5), 1936-1945. https://doi.org/10.1109/JSTARS.2015.2418616.

Trung, N.T., Alemi, N., Haido, J.H., Shariati, M., Baradaran, S. and Yousif, S.T. (2019a), "Reduction of cement consumption by producing smart green concretes with natural zeolites", *Smart Struct. Syst.*, **24**(3), 415-425. https://doi.org/10.12989/sss.2019.24.3.415.

Trung, N.T., Shahgoli, A.F., Zandi, Y., Shariati, M., Wakil, K., Safa, M. and Khorami, M. (2019b), "Moment-rotation prediction of precast beam-to-column connections using extreme learning machine", *Struct. Eng. Mech.*, **70**(5), 639-647. https://doi.org/10.12989/sem.2019.70.5.639.

Unsalan, C. and Sirmacek, B. (2012), "Road network detection using probabilistic and graph theoretical methods", *IEEE T. Geosci. Remote Sens.*, **50**(11), 4441-4453. https://doi.org/10.1109/TGRS.2012.2194158.

Van Engelen, J. E. and Hoos, H. H. (2020), "A survey on semi-supervised learning", *Machine Learn.*, **109**(2), 373-440. https://doi.org/10.1007/s10994-019-05855-6.

Van, E.A., Lindenbaum, D. and Bacastow, T. (2018), "Spacenet: A remote sensing dataset and challenge series", arXiv preprint arXiv:1807.01232.

Visin, F., Ciccone, M., Romero, A., Kastner, K., Cho, K., Bengio, Y., Matteucci, M. and Courville, A. (2016), "Reseg: A recurrent neural network-based model for semantic segmentation", *Proceedings of the IEEE Conference on Computer Vision and Pattern Recognition Workshops*.

Volpi, M. and Ferrari, V. (2015), "Semantic segmentation of urban scenes by learning local class interactions", *Proceedings of the IEEE Conference on Computer Vision and Pattern Recognition Workshops*.

Wang, J., Qin, Q., Yang, X., Wang, J., Ye, X. and Qin, X. (2014), "Automated road extraction from multi-resolution images using spectral information and texture", *2014 IEEE Geoscience and Remote Sensing Symposium*, IEEE.

Wang, J., Song, J., Chen, M. and Yang, Z. (2015), "Road network extraction: A neural-dynamic framework based on deep learning and a finite state machine", *Int. J. Remote Sens.*, **36**(12), 3144-3169. https://doi.org/10.1080/01431161.2015.1054047.

Wang, M. and Luo, C. (2005), "Extracting roads based on Gauss Markov random field texture model and support vector machine from high-resolution RS image", *IEEE T. Geosci. Remote Sens.*, **9**, 271-276. https://doi.org/10.1109/TGRS.2005.848660.

Wang, M., Tan, K., Jia, X., Wang, X. and Chen, Y. (2020), "A deep siamese network with hybrid convolutional feature extraction module for change detection based on multi-sensor remote sensing images", *Remote Sens.*, **12**(2), 205. https://doi.org/10.3390/rs12020205.

Wang, Q., Wan, J., Nie, F., Liu, B., Yan, C. and Li, X. (2018), "Hierarchical feature selection for random projection", *IEEE Transact. Neural Netw. Learn. Syst.*, **30**(5), 1581-1586. https://doi.org/10.1109/TNNLS.2018.2879547.

Wang, S., Guan, K., Zhang, C., Lee, D., Margenot, A. J., Ge, Y., Peng, J., Zhou, W., Zhou, Q. and Huang, Y. (2022), "Using soil library hyperspectral reflectance and machine learning to predict soil organic carbon: Assessing potential of airborne and spaceborne optical soil sensing", *Remote Sens. Environ.*, **271**, 112914. https://doi.org/10.1016/j.rse.2021.112914.

Wang, W., Yang, N., Zhang, Y., Wang, F., Cao, T. and Eklund, P. (2016), "A review of road extraction from remote sensing images", *J. Traffic Transp. Eng.*, **3**(3), 271-282. https://doi.org/10.1016/j.jtte.2016.05.005.

Wei, X., Shariati, M., Zandi, Y., Pei, S.L., Jin, Z.B., Gharachurlu, S., Abdullahi, M.M., Tahir, M.M. and Khorami, M. (2018), "Distribution of shear force in perforated shear connectors", *Steel Compos. Struct.*, **27**(3), 389-399. https://doi.org/10.12989/scs.2018.27.3.389.

Wei, Y., Wang, Z. and Xu, M. (2017), "Road structure refined CNN for road extraction in aerial image", *IEEE Geosci. Remote Sens. Lett.*, **14**(5), 709-713. https://doi.org/10.1109/LGRS.2017.2678380.

Xie, Q., Sinaei, H., Shariati, M., Khorami, M., Mohamad, E.T. and Bui, D.T. (2019), "An experimental study on the effect of CFRP on behavior of reinforced concrete beam column connections", *Steel Compos. Struct.*, **30**(5), 433-441. https://doi.org/10.12989/scs.2019.30.5.433.

Xin, J., Zhang, X., Zhang, Z. and Fang, W. (2019), "Road extraction of high-resolution remote sensing images derived from DenseUNet", *Remote Sens.*, **11**(21), 2499. https://doi.org/10.3390/rs11212499.

Xu, C.H., Zhang, X.L., Haido, J.H., Mehrabi, P., Shariati, A., Mohamad, E.T., Nguyen, H. and Wakil, K. (2019), "Using

genetic algorithms method for the paramount design of reinforced concrete structures", *Struct. Eng. Mech.*, **71**(5), 503-513. https://doi.org/10.12989/sem.2019.71.5.503.

Xu, R. (2016), "A multistage method for road extraction from optical remotely sensed imagery", *J. Inform. Hid. Multimed. Signal Proc.*, **7**(2), 438-447.

Xu, Y., Xie, Z., Feng, Y. and Chen, Z. (2018), "Road extraction from high-resolution remote sensing imagery using deep learning", *Remote Sens.*, **10**, 1461. https://doi.org/10.3390/rs10091461.

Yang, L., Zhuo, W., Qi, L., Shi, Y. and Gao, Y. (2022), "St++: Make self-training work better for semi-supervised semantic segmentation", *Proceedings of the IEEE/CVF Conference on Computer Vision and Pattern Recognition*.

Yang, S., Feng, Q., Liang, T., Liu, B., Zhang, W. and Xie, H. (2018), "Modeling grassland above-ground biomass based on artificial neural network and remote sensing in the Three-River Headwaters Region", *Remote Sens. Environ.*, **204**, 448-455. https://doi.org/10.1016/j.rse.2017.11.018.

Yazdani, M., Kabirifar, K., Frimpong, B.E., Shariati, M., Mirmozaffari, M. and Boskabadi, A. (2020), "Improving construction and demolition waste collection service in an urban area using a simheuristic approach: A case study in Sydney, Australia", *J. Clean. Prod.*, **280**, 124138. https://doi.org/10.1016/j.jclepro.2020.124138.

Yousef Z.A.S.A. and Ramezani, M. (2023), "Advanced integration of IoT and neural networks for real-time structural health monitoring and assessment of bridges", *Int. J. Civil Eng. Adv.*, **1**(1), 1-9.

Zandi, Y., Shariati, M., Marto, A., Wei, X., Karaca, Z., Dao, D. K., Toghroli, A., Hashemi, M.H., Sedghi, Y., Wakil, K. and Khorami, M. (2018), "Computational investigation of the comparative analysis of cylindrical barns subjected to earthquake", *Steel Compos. Struct.*, **28**(4), 439-447. https://doi.org/10.12989/scs.2018.28.4.439.

Zhang, X. and Han, L. (2023), "A generic self-supervised learning (SSL) framework for representation learning from spectra-spatial feature of unlabeled remote sensing imagery", arXiv preprint arXiv:2306.15836.

Zhang, Y., Wang, X., Tan, H., Xu, C., Ma, X. and Xu, T. (2019), "Region merging method for remote sensing spectral image aided by inter-segment and boundary homogeneities", *Remote Sens.*, **11**(12), 1414. https://doi.org/10.3390/rs11121414.

Zhang, Z., Liu, Q. and Wang, Y. (2018), "Road extraction by deep residual U-net", *IEEE Geosci. Remote Sens. Lett.*, **15**(5), 749-753. https://doi.org/10.1109/LGRS.2018.2802944.

Zhou, J., Bischof, W.F. and Caelli, T. (2006), "Road tracking in aerial images based on human–computer interaction and Bayesian filtering", *ISPRS J. Photogramm. Remote Sens.*, **61**(2), 108-124. https://doi.org/10.1016/j.isprsjprs.2006.08.003.

Ziaei-Nia, A., Shariati, M. and Salehabadi, E. (2018), "Dynamic mix design optimization of high-performance concrete", *Steel Compos. Struct.*, **29**(1), 67-75. https://doi.org/10.12989/scs.2018.29.1.067.